Polymer Testing 147 (2025) 108820

Contents lists available at ScienceDirect

Polymer Testing

journal homepage: www.elsevier.com/locate/polytest

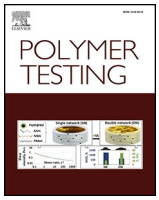

Lifetime prediction and degradation assessment of FKM and FFKM O-rings under high temperature thermo-oxidative ageing

Estefanía Vega Puga [a,b,*], Volker Wachtendorf [c], Anja Kömmling [c], Stefan Brendelberger [a], Matthias Jaunich [c], Christian Sattler [a,b]

[a] German Aerospace Center (DLR), Institute of Future Fuels, Cologne, Germany
[b] Chair for Solar Fuel Production, RWTH Aachen, Aachen, Germany
[c] Bundesanstalt für Materialforschung und -prüfung (BAM), Berlin, Germany

ARTICLE INFO

Keywords:
Fluoroelastomer (FKM)
Perfluoroelastomer (FFKM)
Thermo-oxidative ageing
Lifetime prediction
Compression set

ABSTRACT

To support the development of solar reactor technologies for hydrogen production, this study investigates the thermo-oxidative degradation mechanisms of fluorinated elastomers and predicts their lifetimes at high temperatures (200–300 °C) consistent with the application requirements. An accelerated ageing programme is conducted with FKM and FFKM O-rings and flat samples for up to 21 days. Optical microscopy is used to analyse the exposed seals' morphological changes, while IR microscopy is utilised to investigate the underlying chemical degradation mechanisms of both elastomers. Findings suggest that FKM's degradation arises from dehydrofluorination of the polymer, followed by chain scission and backbone cleavage as a result of the oxidation of newly formed C=C double bonds. FFKM's degradation is primarily associated with chain scission, but there is also indication that post-curing processes may occur during material ageing. Furthermore, hardness, equilibrium compression set (CS), continuous compression stress relaxation (CSR) and leakage rate tests are used to evaluate changes in the mechanical properties and sealing performance of the elastomers. Equilibrium CS data is extrapolated using time-temperature shifts (TTS) and used to derive an end-of-life criterion of 75 % equilibrium CS, which correlates to leakage rates higher than a predetermined threshold. Service lifetime predictions of FKM and FFKM O-rings at several temperatures are performed and a seal operating temperature of 200 °C is suggested, which ensures reasonable O-ring replacement intervals of more than half a year in the solar reactor for both considered materials.

1. Introduction

Fluorinated elastomers are a relatively new grade of synthetic elastomers, extensively utilised across diverse applications such as aerospace, chemical processing and semiconductor manufacturing. These materials exhibit remarkable thermal stability at high temperatures, low permeability to gases and liquids as well as excellent resistance to a broad spectrum of chemicals including mineral oils, aliphatic, aromatic and chlorinated hydrocarbons, acids and weak alkalis [1]. Despite these advantageous properties, fluorinated elastomers, like all polymers, are susceptible to degradation over time when exposed to conditions such as heat, oxygen, radiation, and dynamic loads.

In the context of a recently developed solar receiver-reactor for thermochemical hydrogen production, pressure separation between vacuum and atmosphere at high temperatures is regarded as one of the most critical aspects of this technology's development [2,3]. The solar receiver-reactor operates at high temperatures given the two-step thermochemical cycle it runs, where a reactive redox material is reduced at 1500 °C and subsequently oxidized at 800 °C with water to produce hydrogen. Higher operating temperatures are favoured, as hydrogen production per cycle is increased, thereby enhancing the sun-to-fuel efficiency. The foreseen pressure separation system between reaction zones comprises a gate valve equipped with a high temperature resistance elastomer O-ring. During the transport of the hot redox material between reaction zones, significant radiative heat transfer to the O-ring is expected. Therefore, the gate's O-ring seal is foreseen to operate at temperatures between 200 °C and 250 °C in two media: air and a mixture of water vapour and hydrogen. Depending on the gate design, these temperatures might be exceeded for short periods of time (2 s) in a cyclic repetitive manner. The studied solar receiver-reactor concept is

* Corresponding author. German Aerospace Center (DLR), Institute of Future Fuels, Cologne, Germany.
E-mail address: estefania.vegapuga@dlr.de (E. Vega Puga).

https://doi.org/10.1016/j.polymertesting.2025.108820
Received 8 January 2025; Received in revised form 5 April 2025; Accepted 17 April 2025
Available online 17 April 2025

described in detail in the works of Brendelberger et al. [2] and Vega Puga et al. [3].

For this application, two potential O-ring materials, namely fluoroelastomer (FKM) and perfluoroelastomer (FFKM), have been selected on the basis of their outstanding thermal and chemical resistance characteristics, which align well with the application's requirements. However, available information on FKM and FFKM's sealing performance under thermo-oxidative ageing conditions at high temperatures (200–300 °C) is limited, prompting the need for further investigations in this area. Thermo-oxidative exposure can modify the chemical and physical properties of elastomers, leading to deterioration of the material, which might result in incremental leakage and eventual failure of the entire solar reactor system. Evaluating the ageing behaviour of these elastomers is key in accurately estimating their service lifetime and determining appropriate maintenance schedules for the solar receiver-reactor.

Elastomer lifetime predictions are predominantly based on accelerated thermal ageing, with failure and/or degradation data collected at higher temperatures and extrapolated to service conditions. Kömmling et al. [4–6] conducted accelerated ageing tests on FKM, ethylene propylene diene rubber (EPDM) and hydrogenated acrylonitrile butadiene rubber (HNBR) O-rings at temperatures between 60 °C and 150 °C for up to 5 years to assess the seals' lifetimes. Static and dynamic leakage tests on aged samples were performed and correlated to other properties such as compression set (CS) and compression stress relaxation (CSR). FKM degradation has been studied in a wide variety of environments such as alkaline [7,8] and geothermal [9,10] as well as in contact with oils [11–15] and fuels [16,17]. When considering degradation in air, changes in mechanical properties and chemical structure of aged FKM at temperatures between 150 °C and 200 °C have been analysed and attributed to post-curing and dehydrofluorination [11]. Furthermore, Simon et al. [18] investigated the degradation of a peroxide-cured FKM at 250 °C and concluded that dehydrofluorination occurs as a first step and then chain scission reactions start to take place. The work of Zaghdoudi et al. [19], compared the ageing of FKM in air and hydrogen environments at 150 °C, with the result that degradation in terms of compression set was very similar in both media. Therefore, it was suggested that perhaps the degradation mechanisms of this elastomer are independent of oxygen availability.

Although limited research exists on the ageing and degradation of FFKM, key contributions have been made by the working groups of Sandia National Laboratories and Brookhaven National Laboratory. Studies [9,10] screened the applicability of FKM and FFKM under harsh geothermal conditions and examined CS and their degradation at temperatures up to 300 °C for 24 h in air and 7 days in geothermal brine. At 150 °C in air, the type 1 FKM X-rings showed the least CS (12–17.5 %), while FFKM showed the highest CS (130–220 %) of all tested materials. Furthermore, FFKM displayed an excellent compatibility with the simulated geothermal environments. Reger et al. [20] have established the material service temperatures of several FFKM compounds with different crosslink density by performing 6-week CS tests. Furthermore, the degradation mechanisms of FFKM under thermo-oxidative ageing at 150 °C have been investigated and it was found that network destruction occurs preferentially on the crosslink points of the TAIC curing structure [21].

Existing studies, as reviewed, provide limited results on lifetime estimation under thermo-oxidative ageing of FKM and FFKM elastomers at high temperatures in the range of 200 °C–300 °C. The present work aims to provide further understanding to this relatively underexamined aspect by conducting accelerated ageing tests of elastomeric O-rings and flat sheets at 200 °C–250 °C (FKM) and 250 °C–300 °C (FFKM). The underlying degradation mechanisms of both elastomers were investigated utilising infrared (IR) microscopy. Changes in hardness, CS and leakage rate were determined for samples aged up to 21 days, and continuous CSR tests were performed at 200 °C for 5 months. Furthermore, an end-of-life criterion describing the correlation between a material property and the onset of significant leakage was determined, given that leakage is the only indicator directly linked to seal failure. Lifetime estimates of the elastomeric O-rings at several temperatures were evaluated on the basis of time-temperature superposition and the previously derived end-of-life criterion (75 % equilibrium CS).

2. Materials and methods

2.1. Materials

The formulation of FKM and FFKM elastomers comprises a wide range of ingredients, which affect the final properties of the vulcanizate and the processing behaviour of the compound. An FKM formulation typically includes one or more fillers, an acid scavenger, and a curing system [22]. Generally, 10–30 phr of fillers are employed [23], with potential candidates including carbon black as well as mineral fillers such as silica, barium sulfate, calcium carbonates and calcium metasilicate [24]. Acid acceptors, such as magnesium oxide and calcium oxide, are usually added to counteract the hydrogen fluoride generated during curing or ageing at high temperatures [22]. Fluoroelastomers can be crosslinked by ionic or free radical mechanisms, with bisphenol and peroxide curing being the most used systems up to date. Bisphenol-cured FKMs usually employ Bisphenol AF, an accelerator such as benzyltriphenylphosphoniumchloride (BTPPC) and inorganic bases such as calcium hydroxide and magnesium hydroxide. Peroxide-cured FKMs contain either iodine or bromine-based peroxides usually in conjuction with a triallyl isocyanurate (TAIC) or a triallyl cyanurate (TAC) coagent [24]. Furthermore, plasticizers and processing aids, such hydrocarbon esters, carnauba wax, polyethylene and sulfones, might also be added to improve the processing behaviour of FKM [22]. Some sulfones that are commonly used as processing aids in FKM formulations are diphenyl sulfone (DPS) and dichloro diphenyl sulfone (DCDPS) [25].

FFKM compounds usually include fillers, curatives and processing aids. Potential fillers include carbon blacks, mineral and polymeric fillers [26]. In terms of curing systems, the two more common known systems are peroxide and nitrile cure systems. For peroxide curing, a peroxide initiator such as 2,5-dimethy1-2,5-di(t-butylperoxy)hexane and a coagent such as TAIC or trimethallyl isocyanurate (TMAIC) are usually used, while the possibility of only using a bis-olefin also exists [20,27]. Nitrile-cured FFKMs employ nitrile functional groups in the cure site monomer (CSM) and a proprietary catalyst to form triazine, benzoxazole, and benzimidazole ring structures [20,27]. Similar plasticizers and processing aids as in FKM might be utilised for FFKM compounding, with zinc oxide improving the compression set of peroxide-cured FFKMs [27].

Investigated materials in this study are commercially available FKM with bisphenol curing under the trade name Vi655 [28] and FFKM with peroxide curing under the tradename Perlast G75B [29] supplied by C. Otto Gehrckens GmbH & Co. (Pinneberg, Germany). The exact formulations of the aforementioned elastomers are proprietary, however general compounding details are provided for the readers' reference. The examined FKM is of type 1, composed by vinylidene fluoride (VDF) and hexafluoropropylene (HFP) monomers, and typically exhibits a fluorine content of approximately 66 % [30]. The FKM material has a blue colour, attributed to the presence of an inorganic pigment such as Stan-Tone D-4005 and D-4006 and Cromophtal Blue 4GNP, and titanium oxide (TiO_2), which is often used to stabilize said pigments [24]. Due to the blue colouration of the FKM elastomer, carbon black can be excluded as a filler. The investigated FFKM is made of tetrafluoroethylene (TFE), perfluoromethyl vinyl ether (PMVE) and a cure site monomer, resulting in a fluorine content of over 72 % [27]. Since the FFKM elastomer is black, carbon black is considered among the used fillers. The following Table 1 summarizes the manufacturer's data for the two elastomers used.

Aged samples for each material include O-rings and 2-mm thick sheets. The 2-mm sheets were aged considering that, compared to O-

Table 1
Manufacturer's data for FKM and FFKM materials [28,29].

Material	Minimum Operating Temperature [°C][a]	Maximum Operating Temperature [°C][a]	Hardness [Shore A]		Colour
FKM	−15	200	75 ± 5	DIN ISO 48	Blue
FFKM	−15	325	76	ASTM D2240	Black

[a] Operating temperature in air.

rings, this geometry is more suitable for hardness measurements. The examined O-rings have a cord diameter of 3 mm and an inner diameter of 90 mm. This O-ring geometry has been chosen considering the foreseen application in a solar thermochemical receiver-reactor for fuel production and aiming at obtaining a homogenous ageing of the samples under high temperature thermo-oxidative conditions. A small O-ring cord thickness allows a relative unhindered access of oxygen to the inner areas of the material and thus ensures that the samples are free of diffusion-limited oxidation (DLO) effects. The maximum sheet thickness in which the integrated oxidation across the sample is at least 90 % of the surface equivalent (L_{90}), and therefore minimal DLO effects are present, was estimated to be 7.8 mm for FKM at 200 °C, according to Eq. (1).

$$L_{90} = \left[\frac{k\, p\, P_{ox}}{\phi}\right]^{0.5} \quad (1)$$

where, p is the oxygen partial pressure surrounding the sample, P_{ox} is the oxygen permeability of the sample ($8 \cdot 10^{-7}$ ccsTP/cm · s · cm Hg), ϕ is the oxygen consumption rate ($1 \cdot 10^{-9}$ mol/g · s) and k is a rate constant of 2 considering elastomer ageing in air [31–33]. Since the selected O-rings' cord diameter (3 mm) and flat sample thickness (2 mm) is smaller than L_{90}, all aged samples are assumed to be DLO effect-free. However, it must be noted that the values used for the L_{90} calculation were obtained from literature [31–34] considering a type 1 FKM, and the specific values for the studied material may differ due to a deviating elastomer composition.

2.2. Ageing protocol

FKM and FFKM samples were aged in an oven with fresh air supply according to the DIN ISO 188 standard [35]. Exposure temperatures for FKM are 200 °C, 225 °C and 250 °C, while for FFKM exposure temperatures are 250 °C, 275 °C and 300 °C. The ageing temperatures for each elastomer were chosen with the aim of investigating sealing performance and durability at their corresponding temperature limits. An emphasis on maximizing the operating temperature of the elastomers was given, as being able to operate the seals at higher temperatures would translate into less engineering effort in the design of the pressure system in the solar receiver-reactor. Three O-rings and three flat samples of each elastomer were aged at the respective temperatures to verify the reproducibility of results, and the exposure times are 1, 2, 4, 8 and 14 days. The FKM O-rings at 225 °C were exceptionally aged for an extended period (21 d) to improve the data density of the lifetime estimations. The O-rings were aged compressed in compression set (CS) fixtures with spacers representing a deformation of approximately 25 %, which corresponds to the expected deformation in service. However, it is important to note that the deformation of the O-rings during accelerated ageing at elevated temperature is expected be higher due to the thermal expansion of the elastomers. The O-rings were dismounted from the fixtures and analysed with regard to CS and leakage rate after each exposure time. Silicone oil lubricant was used on the aluminum plates to prevent seal adhesion. The usage of lubricant has a negligible effect on the CS measurements, as reported in literature [8]. After testing CS and leakage rate, the O-rings were mounted again on the fixtures for further ageing under compression in the oven. Once failure of the sealing system was evidenced, where vacuum could no longer be created in the testing volume, the ageing of the O-rings was stopped.

The 2 mm elastomer flat sheets were aged on a perforated metal sheet to ensure hot air circulation. After the hardness measurements at each exposure time were performed on the samples, they were returned to the oven to continue ageing. Care was taken to measure different spots on the sheets each time.

2.3. Analysis methods

2.3.1. Optical microscopy

To observe and document the morphological changes such as appearance, texture and defects of the thermo-oxidatively aged O-rings, optical microscopy was utilised. This non-destructive analysis was performed using a light microscope from Carl Zeiss AG (Oberkochen, Germany) of type SteREO Discovery.V20. The microscope utilises an LED-based reflected light source, has electronic zoom curves and a digital microscope camera (AxioCam).

2.3.2. IR microscopy

In order to follow chemical changes that were affected by the heat exposure including the characterization of heterogeneities, IR microscopy was applied. A device from Bruker Co. (Ettlingen, Germany) of type LUMOS II was utilised. The parameters used are detailed in Table 2.

2.3.3. Hardness

Hardness was measured utilising a Shore A durometer on three stacked 2 mm thick sheets, as per the standard DIN ISO 48-4 [36]. Five positions were measured on the samples at each exposure time, the average value and standard deviation are reported in the Results Section.

2.3.4. Compression set (CS)

The compression set reflects the degree to which an elastomer can recover to its original dimensions after being subjected to a compressive load and is calculated as per Eq. (2).

$$CS = \frac{h_0 - h_2}{h_0 - h_1} \cdot 100\% \quad (2)$$

where h_0 is the initial height of the O-ring, h_1 is the height of the compressed O-ring and h_2 is the recovered seal height. A CS of 0 % represents

Table 2
Parameters used for the IR measurement.

Parameter type	Value
Geometry	ATR
ATR-tip material	Germanium
No. of accumulated scans	Sample: 256, background: 64
ATR tip pressure setting	Medium
ATR-tip cleaning	After each measurement point for heterogeneities like visible spots and lines
Wavenumber range	4000 cm^{-1} to 600 cm^{-1}
IR resolution	4 cm^{-1}
Detector	Liquid nitrogen cooled Mercury-Cadmium-Telluride sensor
VIS lens magnification	8-fold
Sample shape	O-ring, with measurement performed on crest of round-shaped profile
IR sample detection area	Square shaped knife-edge limited aperture, 50 μm width
Corrections used	Atmospheric correction for CO_2 bands. Simple ATR correction. Baseline correction: rubber band
Normalization	No normalization was carried out, neither for FKM nor for the FFKM
Software (acquisition & data manipulation)	Bruker OPUS, version 8.7

full recovery of the O-ring to its original height, whereas a CS of 100 % represents a complete deformation of the seal and absolute lack of recovery. A high CS indicates loss of elasticity and sealing capability, both of which are key in ensuring an optimal seal tightness. The height of each O-ring sample was measured at 8 different locations. According to the DIN ISO 815-1 standard for CS determination at high temperature, Method B, the recovered height (h_2) shall be measured after 30 ± 3 min [37]. However, after this time the recovery of the elastomer is affected by time-dependent viscoelastic effects which could lead to large measurements' inaccuracies. Therefore, in this work, similarly to previous studies [11,12], we employ equilibrium CS values, which facilitate a meaningful assessment of permanent material degradation while minimizing the influence of time-dependent factors. Equilibrium CS values were determined by tempering the samples at 100 °C for 2 h. To confirm that this 2-h tempering does indeed lead to equilibrium values, three samples of each material were tempered for further 6 h. After the second tempering process the CS only changed by a maximum of 2 %. This is a rather small difference considering that after the first tempering CS changed by an average of 10 % and that the error observed for CS measurements of one O-ring is about ±3 %.

2.3.5. Compression stress relaxation (CSR)

Continuous CSR measurements provide information on the loss of sealing force of a compressed seal over time. Measurements were carried out at 200 °C for both FKM and FFKM O-ring segments (length of approximately 45 mm). Three O-ring segments per material were tested for up to 5 months using the stress relaxation rigs EB 02 in a cell oven EB 22 from Elastocon (Brämhult, Sweden) with a compressive strain of 25 % applied at room temperature. Before the start, the samples were first conditioned thermally and mechanically according to the standard DIN ISO 3384 [38]. The force was recorded every 10 s for the first hour, every minute for the next 24 h and afterwards every 10 min (without changing the strain of the sample). The initial force F_0 used for normalization of the values was taken as the force value 30 min after the start of the compression according to DIN ISO 3384 [38].

2.3.6. Leakage rate

The leakage rate of the O-rings aged under thermo-oxidative conditions was experimentally determined in dependence of the ageing time. Leakage rate q was determined utilising the pressure-rise method and is calculated according to Eq. (3).

$$q = \frac{\Delta p \cdot V}{\Delta t} \tag{3}$$

Δp is the pressure change, V is the volume of the vessel where the pressure rise is being recorded and Δt the time elapsed during the test. The leakage rate measurements were performed using the test setup shown in Fig. 1 under ambient conditions. A similar version of this setup has already been introduced by a previous work [39]. The current setup consists of two vacuum chambers, a spacer flange with a groove, where the O-ring is placed, and a custom gate. The custom gate comprises two steel surfaces, a spring in-between them and a linear actuator. The linear actuator is operated to compress the spring which in turn compresses the O-ring being tested. For the leakage rate measurements, first the entire setup (chambers A & B) is evacuated to 0.1 mbar and valve V1 is closed. Then, the custom gate (V2) is closed exerting a force of 445 N on the O-ring. Immediately after, the air vent valve V1 is opened to ambient and the pressure differential between chambers A and B compresses the O-ring further. The O-ring sample can be compressed up to 25 % given the height (2.25 mm) of the groove. The pressure rise in chamber B is recorded for 45 min using an Inficon (Bad Ragaz, Switzerland) pressure sensor (P) with a measuring range from 10^{-4} to 10 mbar and an accuracy of 1 %. Leakage rate measurements were performed using the O-rings that were aged in a compressed state as sealing for the custom gate valve, after performing equilibrium CS measurements. Three measurements on separate samples were completed and the average leakage rate and standard deviation for each ageing temperature and exposure time are calculated.

3. Results and discussion

3.1. Optical microscopy

Microscopy images of the aged O-rings are used to assess morphological changes of elastomers throughout the degradation process. Fig. 2 displays unexposed and thermo-oxidatively aged FKM O-rings at the highest ageing temperature of 250 °C for different exposure times. The highest ageing temperature was selected as it captures the largest extent of observable changes. The unexposed FKM O-ring (Fig. 2 (a)) has an initial blue colour, a circular cross-section and slight surface-porosity. After 2 days of ageing at 250 °C ((Fig. 2 (b)), the O-ring displays a greyish colour, with heterogeneities such as dark spots and lines beginning to appear on the material's surface. These heterogeneities are conserved throughout the ageing process, even after the longest ageing times. Additionally, a flattening of the initially round cross-section is observable, as result of the ageing of the O-ring in a compressed state between metal fixtures. After 8 days of ageing at 250 °C ((Fig. 2(c) and

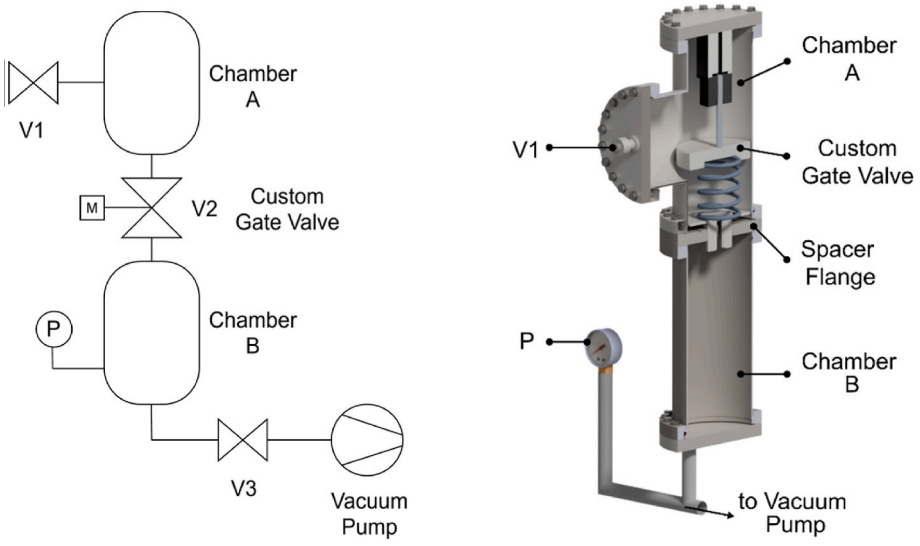

Fig. 1. Schematic diagram and computer-aided design of test stand used for leakage rate measurements.

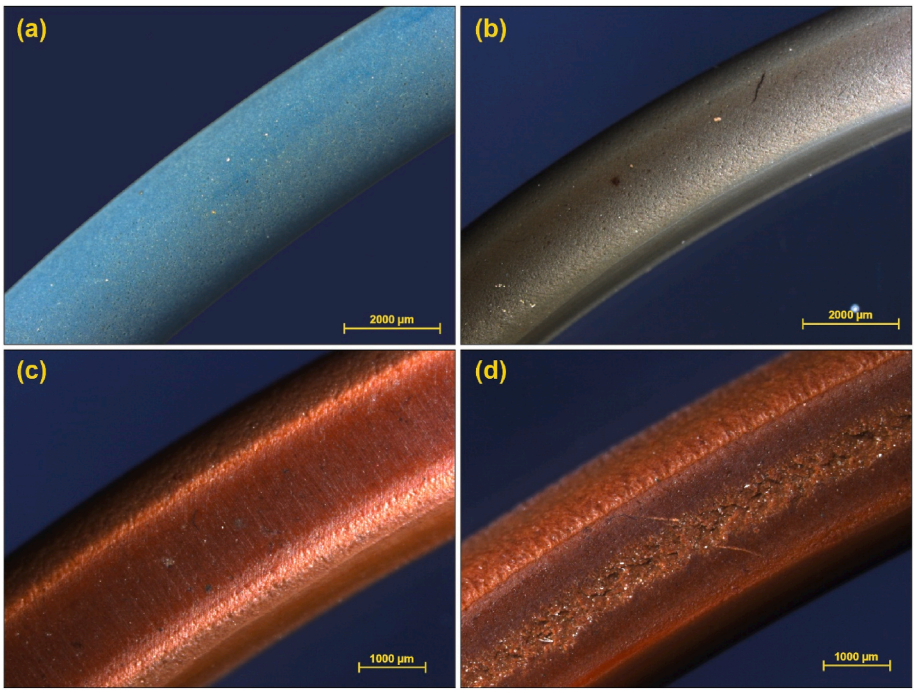

Fig. 2. Optical microscopy images of FKM O-rings under different thermo-oxidative ageing. (a) unexposed, (b) aged at 250 °C for 2 d, (c) aged at 250 °C for 8 d, (d) aged at 250 °C for 8 d displaying a crack.

(d)), the O-rings have undergone further colour changes, now displaying a brownish appearance. The observed colour change may be attributed to the degradation of the blue pigment, polymer degradation involving carbonyl group formation —potentially altering UV–VIS absorption through extended conjugated double bonds—or a combination of both. Filler degradation is regarded as a less likely cause for colour changes, given the thermal stability of the suspected fillers at 250 °C. The flattened area of the O-ring is more apparent and exhibits a series of parallel lines, likely imprints from the surface finish of the metal fixtures, which have left a lasting impression on the elastomer. Furthermore, along the outer diameter of the O-ring, surfaces with increased roughness and irregularities are visible, compared to the smoother compressed sealing face. A possible reason is that the compressive force flattens out developing surface roughness, or that the surface does not become that rough because degradation products cannot leave like on the free surfaces. Another explanation could be the higher exposure of the free surfaces to oxygen, resulting in higher degradation. Additionally, this area experiences the highest tensile stresses from the compression deformation.

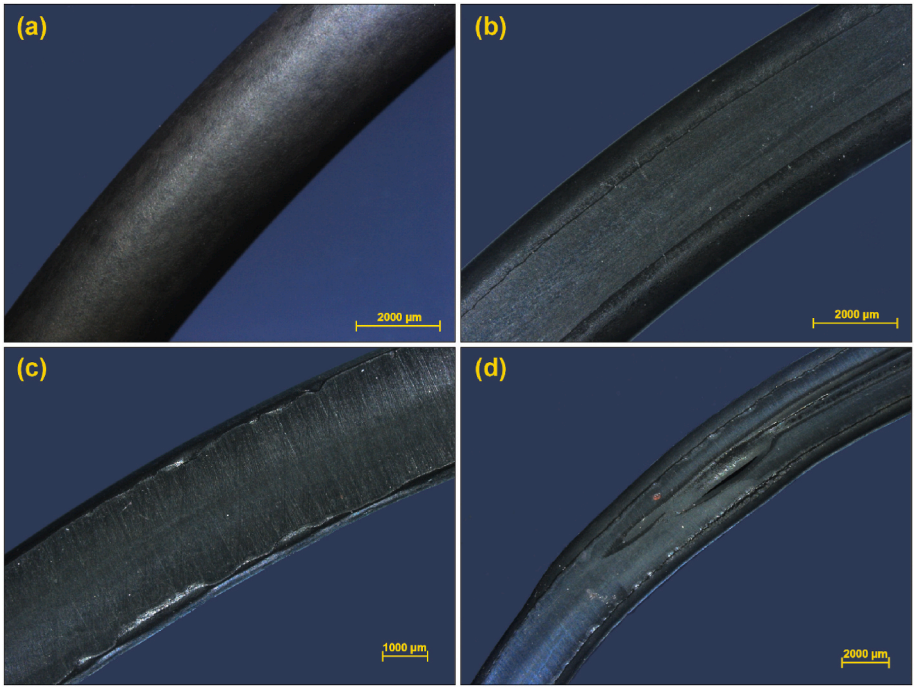

Fig. 3. Optical microscopy images of FFKM O-rings under different thermo-oxidative ageing. (a) unexposed, (b) aged at 300 °C for 2 d, (c) aged at 300 °C for 8 d, (d) aged at 300 °C for 8 d displaying a crack and significant deformation.

Fig. 2 (d) shows an O-ring with a very high roughness in the middle of the sealing area. This is an indication of sticking of the O-ring to the metal surface as a result of chain scission reactions. If the adhesive sticking force is higher than the cohesive forces inside the material, the rubber tears when the O-ring is removed from the flange, leading to the observed roughness. Correspondingly, it was observed that rubber residues remained on the flanges after removing the O-ring.

Optical microscopy images of unexposed and thermo-oxidatively aged FFKM O-rings at 300 °C for different exposure times are shown in Fig. 3. The unexposed FFKMO-ring has a black colour, a circular cross-section and displays less surface-porosity than the unexposed FKM sample. After a 2 day-ageing at 300 °C in a compressed state (Fig. 3 (b)), the O-ring exhibits a flattened cross-section framed by raised material. These lines are situated at the interface region where elastomer, air and the metal fixture meet. After 8 days of ageing at 300 °C (Fig. 3(c) and (d)), the flattened area of the O-ring cross-section increases showing a higher deformation and loss of elasticity of the seal. In this area, similarly to FKM, parallel lines, possibly arising from the metal surface finish, are visible. Furthermore, the edges of the seal face now show larger, irregular material bulges. In Fig. 3 (d) an FFKM O-ring exhibiting larger material degradation and surface distortion after ageing at 300 °C for 8 days is shown. The elastomer seal displays a crack accompanied by an enlarged diameter in the region, suggesting local deformation as a result of the material softening due to chain scission. In this area, the presence of further parallel lines emphasizes the substantial alteration in the O-ring's shape. Next to the crevice in the inner diameter region, a distinct line made up of material bulges is identified, again indicating significant material softening. A small brown spot is evident, presumably metal linked to the peeling of galvanization observed on certain bolts during the test of this particular O-ring.

3.2. IR measurements

Starting with the FKM elastomer (Fig. 4), the results of ATR-measurements on the FKM elastomer as a function of the thermo-oxidative ageing are depicted in Fig. 5. The wavenumber assignments are in accordance with literature [11,18,40,41]. As opposed to these and other authors, no normalization was used, as no definite species that would be invariant to the exposure could be identified. Furthermore, normalization, which is normally used to account for variations in contact between the sample surface and the ATR-tip, was deemed unnecessary in this work. This since, the respective absorbance values across all our measurements, which were later averaged, were consistent and within a small margin of error.

As depicted in Fig. 5 (a), the thermo-oxidative ageing leads to strong changes in the absorption bands around 1085 cm^{-1}. This particular band (1085 cm^{-1}) is associated with CF_2 vibrations. From an initial shoulder for the unexposed FKM, it strongly rises to a peak for ageing at 200 °C for 14 days, stays as such for the sample aged at 225 °C for 14 days, and subsequently diminishes beyond the initial shoulder of the unexposed sample for the sample that was aged for 8 days at 250 °C. Absorptions for CF vibrations at 1394 $cm^{-1}$and for CF_3 at 882 cm^{-1}remain almost unchanged over the ageing at different temperatures.

In agreement with [11,18,40] it is suggested that these changes are the result of the thermally activated elimination of hydrofluoric acid from the $–CF_2$ group of the fluorinated polymer. The elimination leaves behind a C=C double bond, the evolution of which can be followed in Fig. 5, especially in (c). The latter subfigure shows a clear change for an absorption band at 1577 cm^{-1}, which is assigned to the absorption of the C=C double bond. On the stage of C=C double bonds, further crosslinking can occur in competition with their oxidation. For the unexposed sample no shoulder is visible, but for the sample aged at 200 °C a clear peak appears, while for the further aged samples at 225 °C and 250 °C the peak disappeared again. Here, it is suggested that the newly formed C=C double bond readily reacts with oxygen to form oxidized species and hence carbonyl functionalities, such as ketones, aldehydes, acids

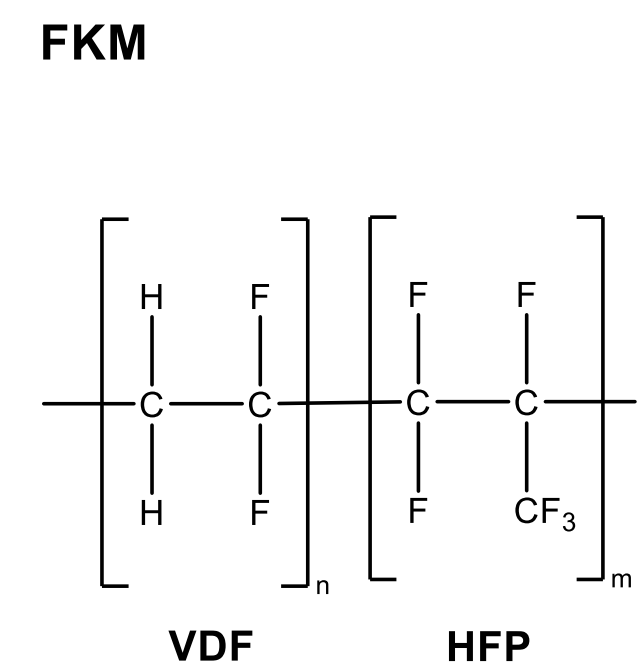

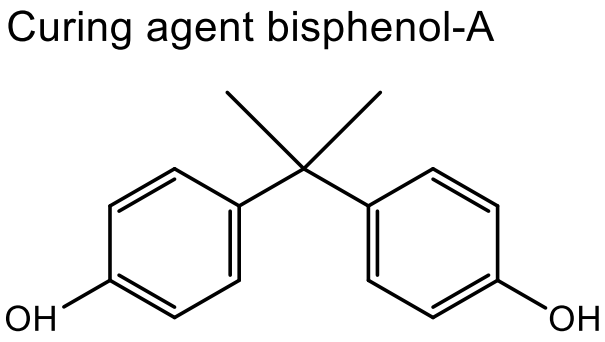

Fig. 4. Schematic chemical structure of monomers and curing agent present in the tested FKM polymer.

and esters are formed, which indeed are visible in the area 1700 cm^{-1} to 1850 cm^{-1}. As this once again is a thermally activated process, it does not surprise that the shoulders at 1719 cm^{-1}, 1751 cm^{-1}, and 1786 cm^{-1} are highest for the highest ageing temperature of 250 °C and second highest for the second highest ageing temperature of 225 °C. Whereas, for the sample aged at 200 °C and the unexposed one only a low basic absorption is visible for this region (probably due to the prior thermal fabrication history of the sample) on top of which the before mentioned extra absorption are superimposed. The oxidation of C=C double bonds to carbonyl species is associated with chain scission and backbone cleavage, which will lead to a deterioration of mechanical strength [21].

The absorption of C=C double bonds at 1577 cm^{-1} compared to unexposed first runs through a maximum at 200 °C and subsides afterwards (Fig. 6 (b)). This phenomenon is explained by the fact that the formation of C=C double bonds and the consumption of double bonds in favour of their oxidation or by the formation of C–C crosslinks are competing processes, and their balance is temperature dependent. In the lifetime of double bonds, these have a third competing reaction, which consists in crosslinking, accounting from the reaction of two double bonds. However, this is intrinsically difficult to observe in the IR spectrum as usually only subtle changes, rather than new peaks, result. Principally in the early heating stages, post-curing reactions might

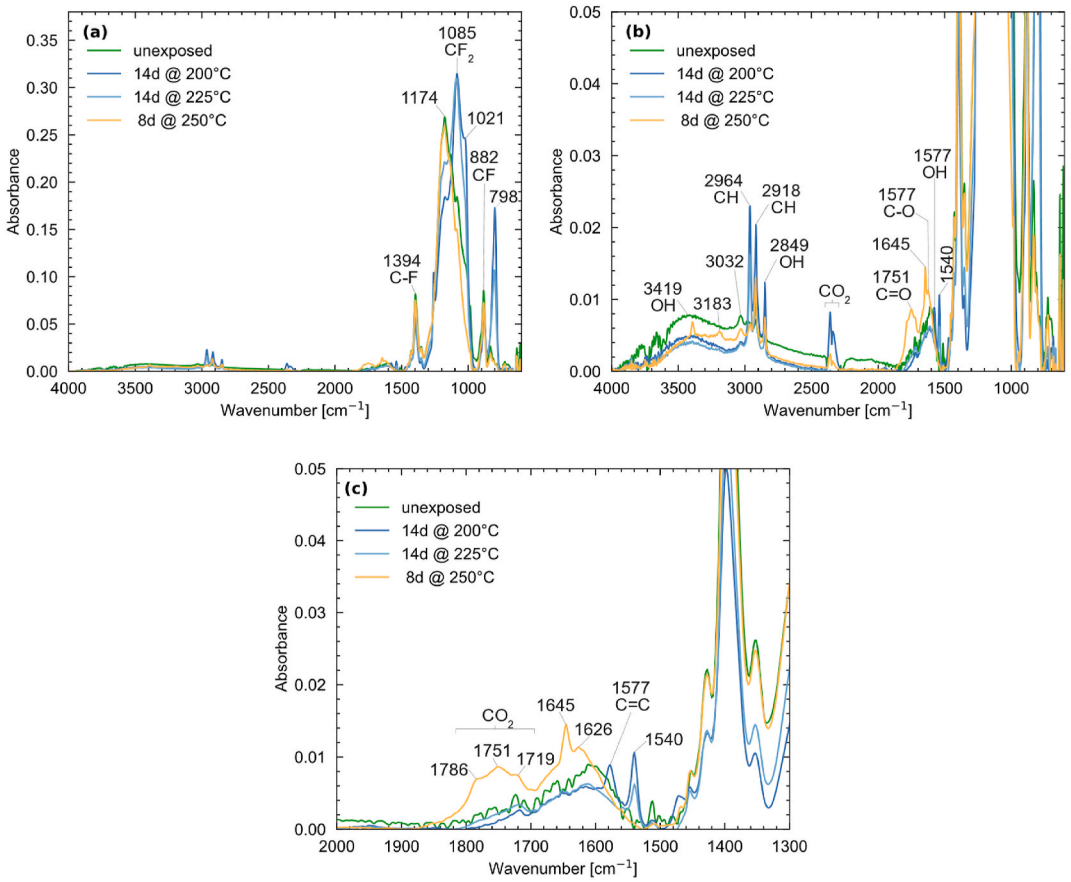

Fig. 5. ATR-IR spectra of thermo-oxidatively aged FKM as a function of ageing temperature and duration, (a) with wavenumber ranging from 4000 cm^{-1} to 600 cm^{-1}, (b) with enlarged absorbance axis, (c) with reduced wavenumber ranging from 2000 cm^{-1} to 1300 cm^{-1}.

occur. The different development of carbonyl, C=C double bonds and CF_2 groups in terms of their respective peak area (which is proportional to the concentration of the respective group) are depicted in Fig. 6. The procedure for evaluating the peak area with subtracting the baseline below the peak is shown exemplarily in Fig. 6 (d). An overview of the proposed degradation mechanism of FKM with thermo-oxidative ageing is depicted in Fig. 7.

Apart from following IR changes in the FKM samples as a function of ageing, also the significance of dark spots and lines in contrast to their unspotted environment was investigated. FKM lines and spots for samples exposed for 8 d at 250 °C are shown in Fig. 8. For the IR-comparison of the structures of dark lines and spots, their homogeneous brownish environment, and the unexposed sample, no normalization could be found that would fit all samples. Therefore, the comparison was conducted with the absolute absorbance.

Fig. 9 shows different wavenumber regions for the comparison of the unexposed sample and the different locations of the 250 °C aged sample. The spot 1 region shows good agreement with the brownish homogeneous surrounding, while the dark line also still shows similarities with only less concentration of species in the CF_x region and higher concentration in the carbonyl region. The spot 2, on the other hand, is different in both wavenumber regions and does not seem to show any sort of thermal-oxidative generated transformation product, but rather is a different sample. A library search indicated that this substance is a poly (dimethylsiloxane), PDMS, rubber with high probability [42], which could have been used as lubricant during the rubber production. The associated PDMS absorptions are marked as the respective Si-bond labels within the data labels in Fig. 9 (b).

For the FFKM elastomer, its chemical structure is shown in Fig. 10 and the results of the ATR measurements are summarized in Fig. 11. As in the case of the FKM, no normalization was used. Main peak assignments are adapted from Ref. [43] for the unexposed sample, from Ref. [21] for the thermo-oxidatively aged FFKM and from Ref. [44] for the perfluoromethylvinylether (PMVE). As visualized in Fig. 11 (a), the main chemical change effected by ageing occurs in the wavenumber region of about 900 cm^{-1} to 1300 cm^{-1}, which is associated with different C–F bonds. This area is shown in more detail in Fig. 11 (b). The main peaks showing at 1202 cm^{-1} and 1150 cm^{-1} for the unexposed FFKM with initial highest absorption for the CF_2 are typical for a poly (tetrafluoroethylene). For the ageing at 250 °C these peaks are significantly lowered and still lower somewhat further for 275 °C and 300 °C. It is suggested that a thermally driven elimination of CF_2 groups occurs which leads to the lowering of the two absorption bands. The loss of CF_2 fragments must be associated with a C–C bond break in the main chain forming radical fragments and the possibility of molecular re-arrangements (and hence means a deterioration of mechanical strength).

With increasing ageing temperature, a shoulder at 1085 cm^{-1} emerges for the 250 °C sample which then only weakly grows for the 275 °C and 300 °C samples. In the difference spectrum (300 °C minus unexposed) the shoulder shows as a peak at 1085 cm^{-1}, which could be associated with C–O–C or C–F_x bonds. Hiltz [45] examined pyrolysis GC/MS results at temperatures between 700 °C and 900 °C for a somewhat different fluoroelastomer (a terpolymer from hexafluoropropylene (HFP), tetrafluoroethylene (TFE), perfluoromethyl vinyl ether (PMVE) and vinylidene fluoride (VDF), hence also containing C–H bonds). He proposed that an $^{+}\bullet OCF_3$ fragment is eliminated from the original ether bond of the PMVE segment and that the majority of degradation products are associated to the PMVE part of the polymer. In our case, this might be responsible for the shoulder at 1085 cm^{-1}. As

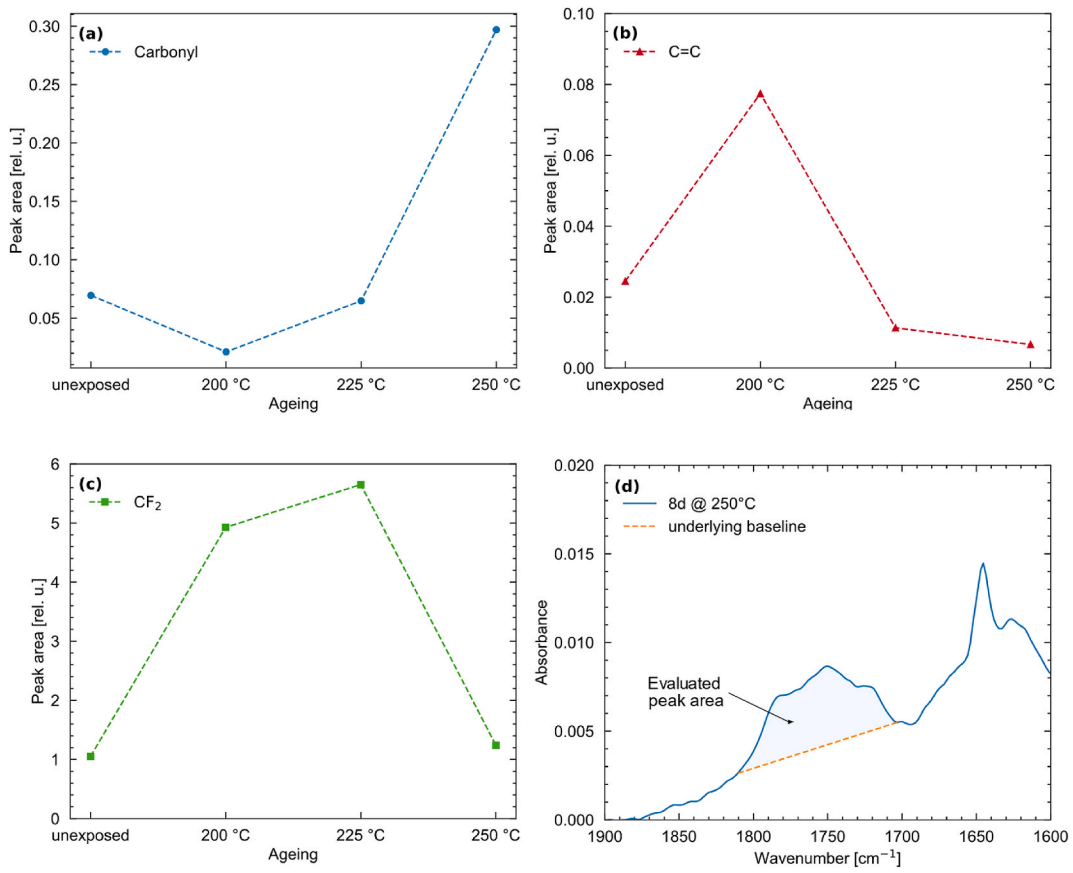

Fig. 6. Ageing dependent development of peak area (corrected for the underlying baseline) in FKM for (a) carbonyl within 1703 cm^{-1}–1810 cm^{-1}, (b) C=C double bond within 1562 cm^{-1}–1600 cm^{-1}, (c) CF_2 groups within 1040 cm^{-1}–1150 cm^{-1}. (d) Graphical explanation of procedure used for peak area evaluation for the example of the carbonyl area between 1703 cm^{-1} and 1810 cm^{-1} of the FKM aged for 8 days at 250 °C.

ideally no hydrogen is present in the perfluorinated molecule, no elimination of hydrofluoric acid, HF, in the associated formation of C=C double bonds is observed. The increase of the absorption band around 798 cm^{-1} (788 cm^{-1} for the unexposed) from unexposed to 300 °C is attributed to CF_2 groups.

The change of weak bands is depicted in Fig. 11 (c). Here, very weak absorptions of CH_2– and CH_3–vibrations are detected (mind the highly expanded y-axis scaling), which should not exist for an ideally perfluorinated polymer, but most probably are due to crosslinking agents. These decrease systematically in the series from unexposed to 300 °C ageing and might be an indication of post-cure processes. A similar trend is observed for the 1714 cm^{-1} carbonyl absorption as well as for the OH absorption band around 3400 cm^{-1}, all of which, are suggested to belong to an additional component like the cure site monomer. While changes in the chemical composition were observed in the IR spectra and described above, their significance for mechanical changes will be discussed in the following sections. An overview of the proposed degradation mechanism of FFKM is detailed in Fig. 12.

3.3. Hardness measurements

Hardness of FKM and FFKM materials was measured on three stacked 2-mm thick sheets before thermo-oxidative ageing was undertaken and after several exposure times. Unexposed FKM samples have an average hardness of 75.8 Shore A, while unexposed FFKM ones have a hardness of 85 Shore A, showing a value higher than the one given by the manufacturer. Hardness measurements of aged samples of both materials at several temperatures and exposure times are graphed in Fig. 13. For FKM a slight increase in hardness is observed with longer ageing times and higher temperatures. This could be attributed to post-curing reactions and degradation or loss of plasticizers and lubricants which represent approximately 0.25 wt% of the material, as reported in literature for similar investigations conducted at lower temperature ranges (75–150 °C) [6]. The cage effect, characteristic of heavily fluorinated polymers, likely mitigated the hardness increase of aged FKM samples. This effect constrains free radical mobility and facilitates their recombination within the fluoropolymer matrix, effectively inhibiting the propagation of degradation reactions and minimizing permanent structural damage [46–48]. However, it is important to note that at higher temperatures, where the chain mobility is largely increased, radicals are no longer able to recombine leading to enhanced material degradation [47]. To validate the hypothesis that post-curing during thermo-oxidative ageing leads to increased hardness in FKM, future studies could directly measure the crosslinking degree of aged samples, providing quantitative evidence for this proposed mechanism.

In the case of FFKM, an opposing trend to FKM is observed, as hardness decreases significantly with increasing ageing temperature and exposure time. The identified decrease in hardness could suggest dominant chain scission reactions as the elastomer ages, coinciding with the degradation mechanism (C–C bond break in the main chain) identified from IR measurements. Additionally, a previously conducted study examining thermo-oxidative ageing of peroxide cured FFKM at temperatures between 90 °C and 150 °C suggests that degradation arises from two simultaneously occurring processes: post-curing and destruction of the TAIC crosslinking structure (peroxide curing coagent), with the latter being dominant at higher temperatures [21]. Furthermore, due to the higher ageing temperatures of FFKM, recombination of free radicals might have been hindered by increased molecular mobility. At the highest FFKM ageing temperature (300 °C) and longest time (8 d) a large decrease in hardness is observed. This measurement is also

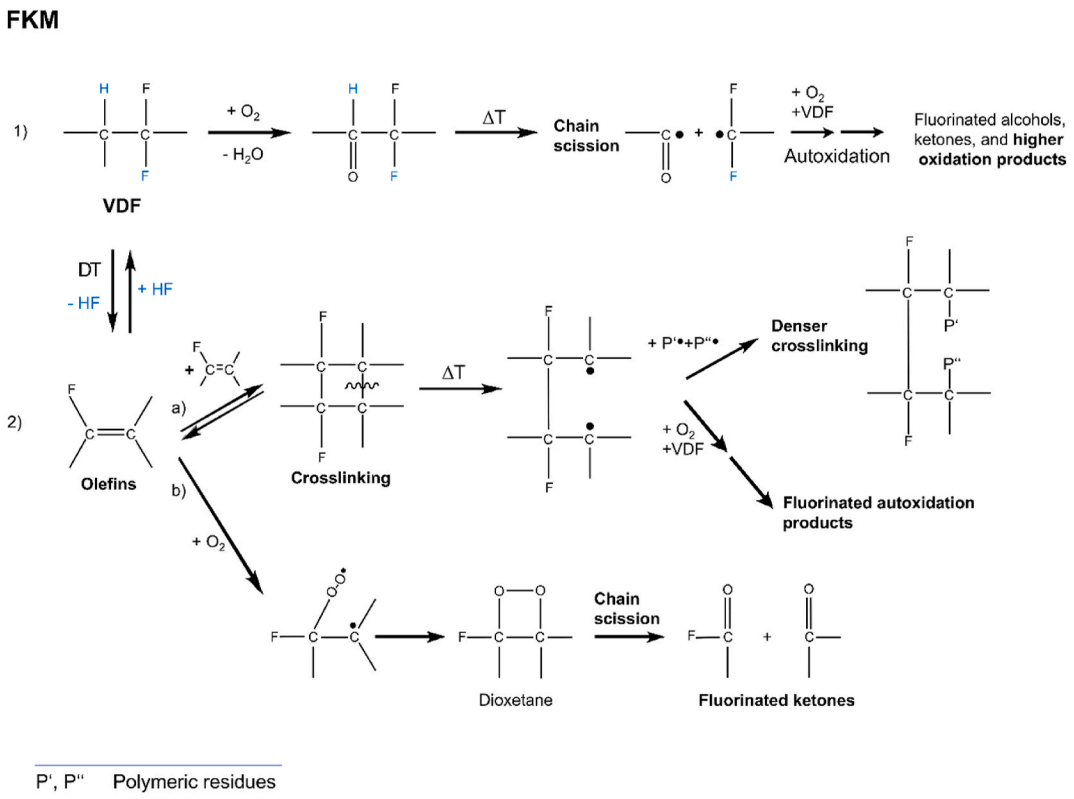

Fig. 7. FKM proposed reaction scheme. 1) Either elimination of HF out of the VDF part of the macromolecule leads reversibly to fluorinated olefins or autoxidation of the VDF component can lead to oxidized products. 2) The fluorinated olefins can react either with themselves reversibly leading to crosslinking or react with oxygen forming dioxetane, the scission of which results in fluorinated ketones and chain scission.

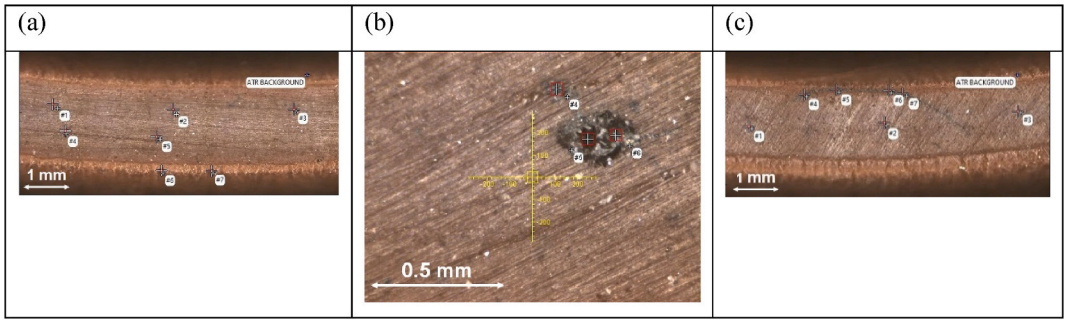

Fig. 8. Locations and ATR-IR measurement positions of the 3 heterogeneities: (a) line, (b) spot 1 with micrometre scale as yellow crosshair, and (c) spot 2. This is the same sample shown in Fig. 2 (c), differences in colour are attributed to the different microscopes and white balances used.

associated with a large measurement uncertainty since the samples were adhered to the perforated metal sheet on which they were aged. Therefore, on the surface of the samples a pattern corresponding to the geometry of the perforated metal sheet could be distinguished and depending on which area of the sample the hardness was tested, a different value was obtained.

3.4. Equilibrium CS measurements

Measured equilibrium CS values for aged FKM and FFKM O-rings at several temperatures and exposure times are shown in Fig. 14. Both materials, FKM and FFKM, show an increase in CS with increasing temperatures and longer exposure times. However, FFKM exhibits a moderately high CS even after only 1 d of ageing across all tested exposure temperatures. This observation is notable given that the ageing tests were conducted below the manufacturer's specified maximum temperature, while the FKM tests were performed at temperatures beyond its maximum specified temperature. Additionally, it is important to consider that the CS measurements were performed on O-rings that were aged compressed in CS fixtures with a deformation of 25 %. This 25 % deformation was performed at ambient conditions, before the compressed samples were heated in the oven. Given that the coefficient of thermal expansion of FFKM is reported to be significantly higher (30 % more) than that of FKM at the same filler loading [27], and the FFKM samples were heated to 50 °C higher temperatures than the FKM samples, the FFKM O-rings would have experienced a greater deformation at elevated temperatures in the oven due to thermal expansion of the elastomer material. This increased compression results in larger stresses that could potentially lead to a higher initial CS. For instance, at the temperature of 250 °C, after 1 d of exposure, FKM exhibits better recovery properties than FFKM, with a slightly lower CS. However, at the same ageing temperature but at longer exposure times (>2 d) FKM's CS becomes larger than that of FFKM. The significantly higher CS observed in FKM indicates it is more degraded than FFKM, thereby confirming the

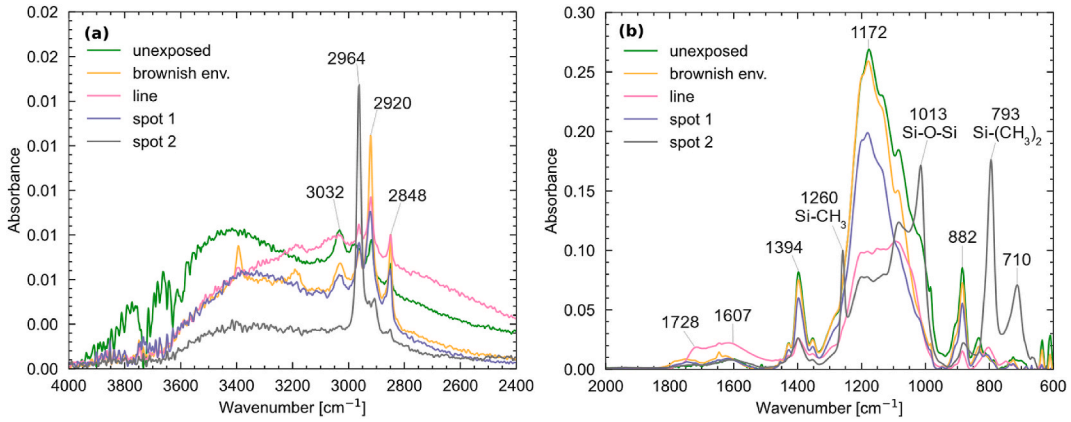

Fig. 9. ATR-IR spectra of FKM aged for 8 d at 250 °C. Investigation of brownish homogeneous region compared to dark line, dark spots and unexposed sample, (a) in the wavenumber region 4000 cm^{-1} to 2400 cm^{-1}, (b) in the wavenumber region 2000 cm^{-1} to 600 cm^{-1}.

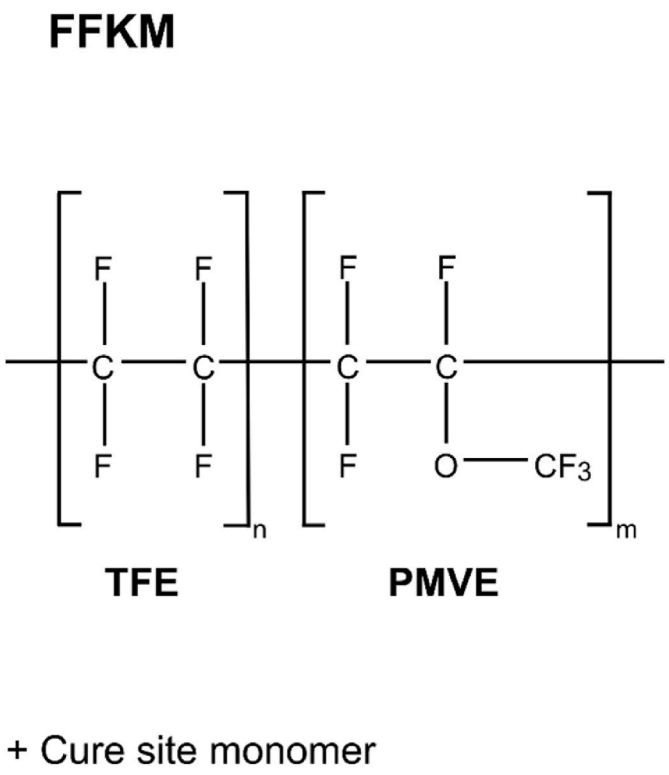

Fig. 10. Schematic chemical structures of monomers present in the tested FFKM polymer.

superior temperature resistance of the latter. To reduce the CS of FFKM, an initial O-ring compression of 18 %, which would result in approximately 25 % compression at 325 °C, could be applied [20]. However, for the purposes of this study, the use of standardized compression values to determine CS in line with DIN ISO specifications was deemed more appropriate.

Moreover, it should be noted in the case of both elastomers, CS values show a much more prominent material degradation than hardness. For example, in the case of FKM exposed at 250 °C for 14 d, hardness shows a moderate increase by 3 Shore A points, while for equilibrium CS a 95 % loss of resilience is evidenced. An effect that could potentially contribute to CS showing more material degradation than hardness is the previously discussed cage effect (Section 3.3), in which free radicals recombine and lead to a reduced permanent damage [48]. In the case of flat samples used for hardness testing, this recombination might have been more pronounced than in the O-rings used for CS measurements given that they were aged under compression and thus subjected to larger stresses. Consequently, in the case of the compressed O-rings, the ends of the fragmented chains may have relaxed and moved apart, preventing recombination. These chain ends are likely to interact with other chains, thereby exacerbating the degradation process. Another less likely explanation for this is the simultaneous occurrence of chain scission and crosslinking (due to post-curing processes) during thermo-oxidative ageing, whose effects can balance each other out when measuring hardness, but have an additive effect on CS [49–51]. In general, chain scission reactions reduce hardness, while crosslinking tends to increase it. Therefore, the overall measured surface hardness change is given by the reaction that dominates and does not necessarily reflect the full extent of the material's degradation. On the other hand, CS increases as a result of both chain scission and crosslinking, since chain scission leads to fractured bonds that are unable to participate in recovery, and additional crosslinking during ageing fixes the deformed O-ring geometry by creating new bonds [19].

3.5. CSR measurements

Compression stress relaxation (CSR) tests were performed on FKM and FFKM O-ring segments at 200 °C. Fig. 15 displays the force (F) normalized with respect to the elastomers' initial sealing force (F_0) over the ageing time, shown in logarithmic and linear scales. Three curves per material corresponding to the tested samples are graphed. One FKM and one FFKM measurement were stopped after approximately 2 months, both due to technical errors of the testing equipment. A decrease in sealing force is observed over ageing time for both elastomers, with a fast force decline at first (on the linear time scale), which transitions to a slower decrease as the ageing time progresses. Previous studies affirm that the initial force reduction is correlated to physical relaxation of the elastomers (e.g. relaxation of polymer chain units or movement of entanglements), while the more dominant force decrease at the later stage is associated with chemical relaxation (e.g. oxidative chain scissions) [51–53]. Our experimental results show that FFKM has a slightly larger relaxation in the initial physical phase, while FKM exhibits higher relaxation in the chemical phase. The pronounced force decrease of FKM at longer ageing times is associated with the degradation of the polymer structure as thermo-oxidative ageing progresses. Certainly, FFKM displays a superior resistance to thermal degradation at 200 °C by conserving more sealing force at longer exposure times.

CSR results further validate equilibrium CS findings, with FKM displaying an inverse correlation between CSR and CS. However, this comparison could not be made for FFKM as the CSR testing temperature (200 °C) is lower than the ageing temperatures used for equilibrium CS. The 200 °C temperature limitation arises from the experimental

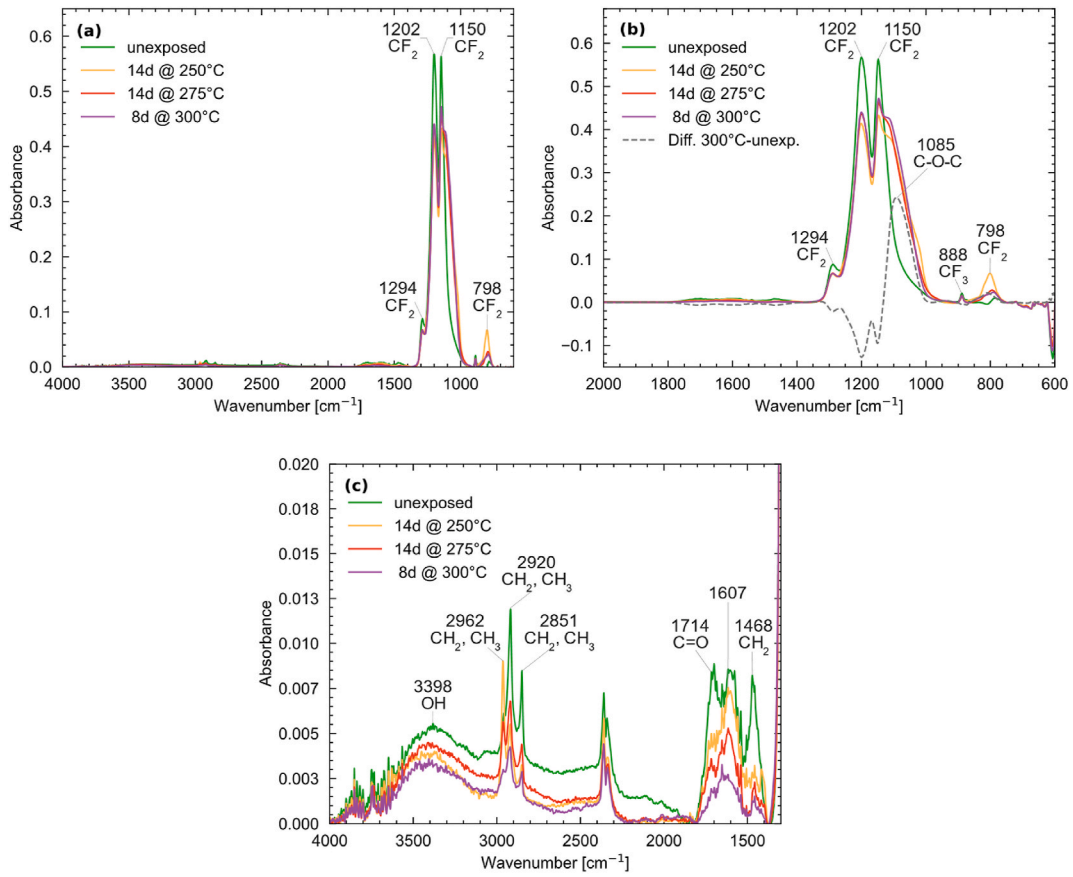

Fig. 11. ATR-IR spectra of thermo-oxidatively aged FFKM as a function of ageing temperature and duration, (a) in the wavenumber region 4000 cm^{-1} to 600 cm^{-1}, (b) in the wavenumber region 2000 cm^{-1} to 600 cm^{-1} additionally calculated difference spectrum between aged at 300 °C and unexposed sample shown as dashed line, (c) in the wavenumber region 4000 cm^{-1} to 1300 cm^{-1}.

equipment used in CSR testing. Similar to CS, CSR indicates greater material degradation than hardness, as the sealing force decreases in an additive manner through chain scission and crosslinking reactions, and the cage effect may not be as effective for ageing in the compressed state. Consequently, CS and CSR exhibit greater sensitivity to material degradation compared to hardness measurements, making them a more reliable indicator of structural changes and thus better suited for accurate lifetime prediction of sealing components.

3.6. Leakage rate

Leakage of a fluid through an elastomeric seal can arise from permeation through the elastomeric seal and secondary leakage, which results from the existence of leakage channels at the interface between the seal and the mating surface. In a sealing system, leakage is the only characteristic directly correlated with seal failure, which can provide a reliable end-of-life criterion for the O-rings. Therefore, the leakage rate of thermo-oxidatively aged FKM and FFKM O-rings at various exposure times and temperatures was measured and is reported in Fig. 16. Since leakage is inevitable under real-world conditions, a technical leak tightness is usually defined as a maximum allowable leakage rate according to the operation in question [54]. In this work, the maximum allowable leakage rate or threshold leakage is defined as one order of magnitude increase of the leakage rate of the unexposed O-rings and is represented by a black dash-dotted line in Fig. 16. This threshold was chosen because a tenfold increase in leakage rate can significantly affect the solar receiver-reactor's performance, and it is also a criterion commonly applied in vacuum technology, which indicated a considerable change in performance [55].

In the present work, failure of FKM is associated with a leakage rate of $2.2 \cdot 10^{-3}$ Pa m^3/s (21 d of ageing at 225 °C), which is well above our predefined threshold leakage and represents an increase of two orders of magnitude from the leakage rate of the unexposed O-rings. Likewise, for FFKM O-rings failure occurs at a leakage rate of $8.9 \cdot 10^{-4}$ Pa m^3/s (4 d of ageing at 300 °C). Leakage rate measurements of FKM O-rings aged 8 d at 250 °C and FFKM O-rings exposed at 300 °C for 8 d were attempted, but no vacuum could be established. Failure of the O-rings occurred in a sudden manner, rather than progressively. Similar observations, in terms of O-ring failure during thermo-oxidative ageing, have been reported in previous research [5,47,56].

For both materials, a variability in leakage rate is evidenced over the course of the ageing process. This measurement variability may initially suggest a decrease in material permeability as a potential cause, however based on a previous study [19] in which the permeability of FKM did not change when aged at 150 °C for up to 100 days, and considering that the dominant degradation mechanism of FKM and FFKM is chain scission, this explanation is unlikely. Therefore, it is probable that the leakage rate measurement variability arises from the test procedure and setup used, in which outgassing of the O-rings and several components' seals might have influenced the results, as well as differing ambient temperature and pressure during the measurements.

Prior investigations [5,47,56,57] have shown that despite extensive material degradation, elastomer O-rings can remain leak-proof due to adhesion of the seal to the mating surface. However, this adhesion of the seal under static conditions is not representative for dynamic applications, where the contact between seal and mating surface is repeatedly broken. Therefore, in this study, compressed O-rings were aged in lubricated fixtures from which they were carefully removed in order to proceed with leakage testing. This approach ensures that no adhesive effects influenced the results and might have led to high leakage

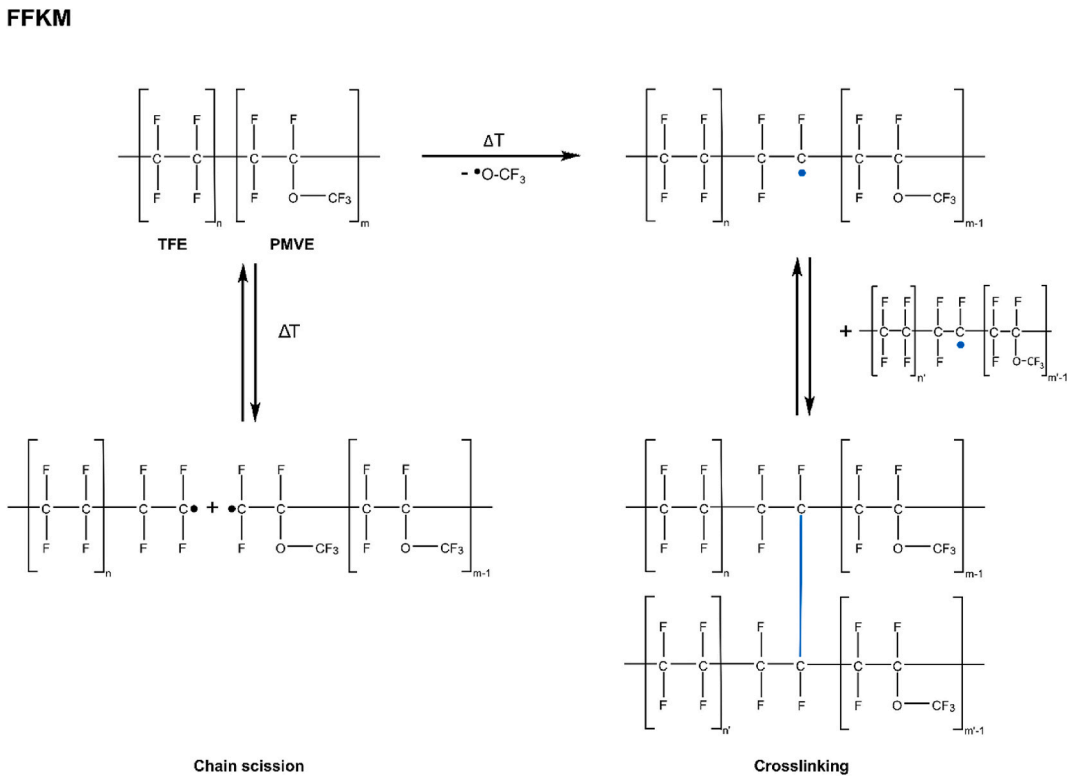

Fig. 12. FFKM proposed reaction scheme. Either the elimination of a trifluoromethylether radical out of the PVME section of the FFKM leaves a polymer radical that can reversibly react with itself to form a crosslinked product. Or the split of a C-C carbon bond leads to two radicals meaning chain scission.

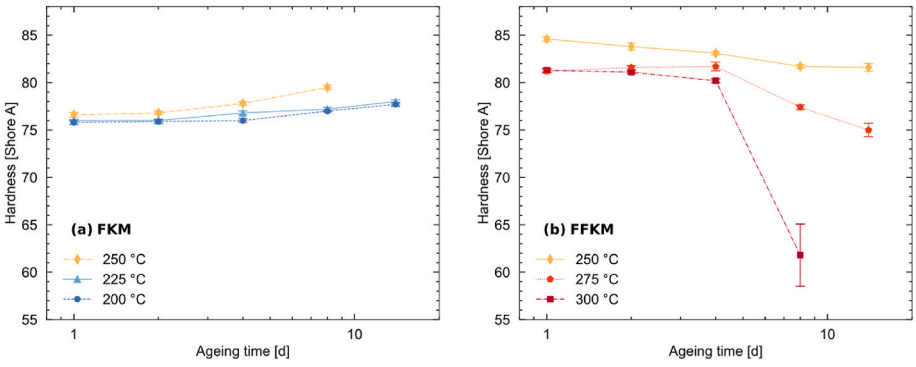

Fig. 13. Shore A hardness of a) FKM and b) FFKM flat samples with respect to aging time.

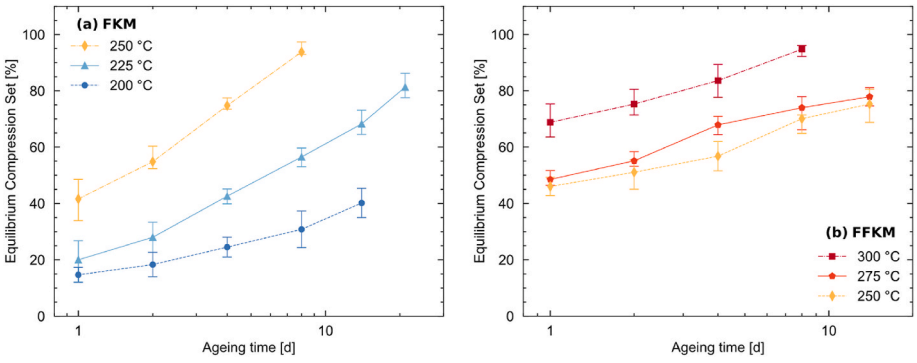

Fig. 14. Equilibrium compression set measurements of aged (a) FKM and (b) FFKM O-rings.

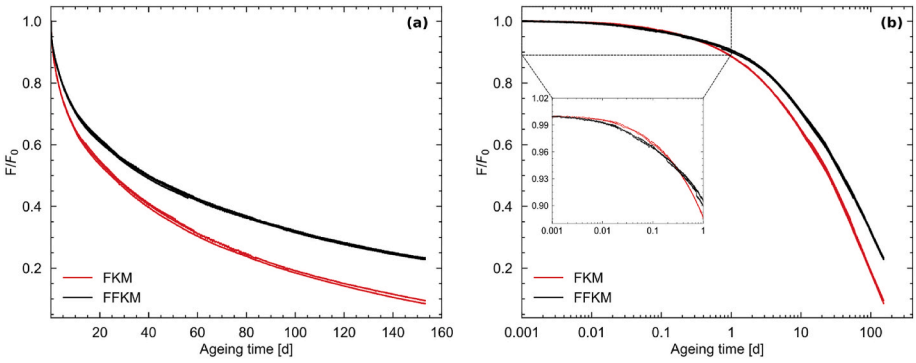

Fig. 15. Compressive stress relaxation of FKM and FFKM O-ring segments at 200 °C, (a) linear time scale, (b) logarithmic time scale.

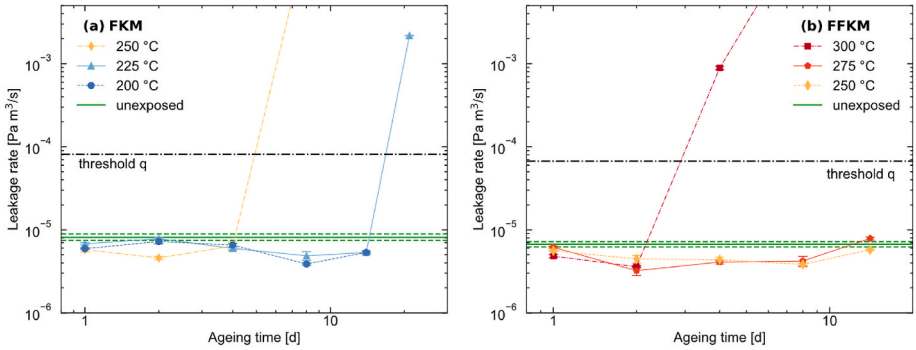

Fig. 16. Leakage rate of aged O-rings for (a) FKM and (b) FFKM. The error range of the leakage rate measurement of the unexposed O-rings is shown as dashed green lines. Threshold leakage is represented by a black dot-dashed line. In the tests were the system could not be evacuated to 1 mbar, the leakage rate is assumed to be infinite and depicted out of the diagram box.

occurring at lower material ageing states than those found in literature [5,47,56,57], thus presenting a more conservative and accurate evaluation of leakage rate as an indicator of seal failure for dynamic applications.

3.7. Lifetime prediction

For the estimation of the lifetime of FKM and FFKM O-rings in the examined application, the time-temperature superposition (TTS) method is utilised. Unlike other methods such as the Arrhenius approach, the TTS has the advantage that all the time-dependent data generated at each ageing temperature are used, leading to a more accurate lifetime prediction [58,59]. A master curve at a reference temperature, usually the lowest tested temperature, is developed by shifting the higher temperature data sets on the logarithmic time axis until superposition is achieved. The constant factor by which the higher temperature ageing times are multiplied is known as the shift factor (a_T) and it is empirically derived to provide the best overall data superposition. In this work, equilibrium CS measurements are utilised for TTS as this method is particularly sensitive to material degradation as discussed in Section 3.4, and more data was available compared to the equally suited CSR. FKM and FFKM equilibrium CS master curves and shift factors are shown in Fig. 17. Additionally, the measured leakage rates corresponding to the shifted times are also plotted on the secondary axis. This helps to establish a correlation between the leakage rate of an O-ring at a determined ageing state and its CS. The reference temperature of FKM is 200 °C, while for FFKM it is 250 °C, on account of their ageing temperatures.

Equilibrium CS data of both materials allow a good superposition in the measured time and temperature ranges. Failure of the O-rings, when the leakage rate is higher than the predefined threshold, is evidenced when CS is approximately 81 % for FKM and about 83 % for FFKM. Adjacent measurements, where the O-rings were still leak tight, display CS values of 75 % and 78 % for FKM and FFKM respectively. Consequently, 75 % CS is conservatively selected as end-of-lifetime criterion for both elastomers. Previous research [4,5] found that 80−85 % equilibrium CS is suitable end-of-life criterion for aged EPDM O-rings, when considering dynamic leakage tests involving a fast and small partial decompression of the seals after static ageing with no disassembly of the seal. The lower, more conservative, end-of-life criterion found in the present study might be attributed to the fact that ageing of the O-rings was repeatedly interrupted to perform characterization tests on the samples. Since the O-rings were frequently removed from the fixtures and thus seal adhesion was hindered, high leakage rates might have been evidenced at lower material degradation levels than in other investigations.

Plotting the logarithm of the shift factors and the inverse temperature (Fig. 18) permits an Arrhenius type analysis of the underlying degradation mechanism of the investigated elastomers. If the data points can be connected by a single straight line, it can be assumed that no changes in the dominant reaction mechanism occur within the studied temperature range. In the case of the FKM's data set, a highly satisfactory linear fit could be applied, and an apparent activation energy (E_a) of 116 kJ/mol was determined. This value is higher than published data, where an E_a of 78 kJ/mol for bisphenol cured FKM was found using equilibrium CS data in a temperature range of 75–150 °C [4]. Another study found an E_a of about 82 kJ/mol using stress relaxation for an FKM of type 2 between 150 °C and 275 °C [60]. A recent report using the "power law" model found E_a in the range of 117–151 kJ/mol for an FKM O-ring with end -of -life criteria in the range of 50–80 % CS at temperatures between 100 °C and 200 °C [61]. The deviations evidenced for the calculated E_a of FKM can be attributed to the different testing methods employed, as they significantly impact the outcome, and therefore a direct comparison of the mentioned activation energies is not possible

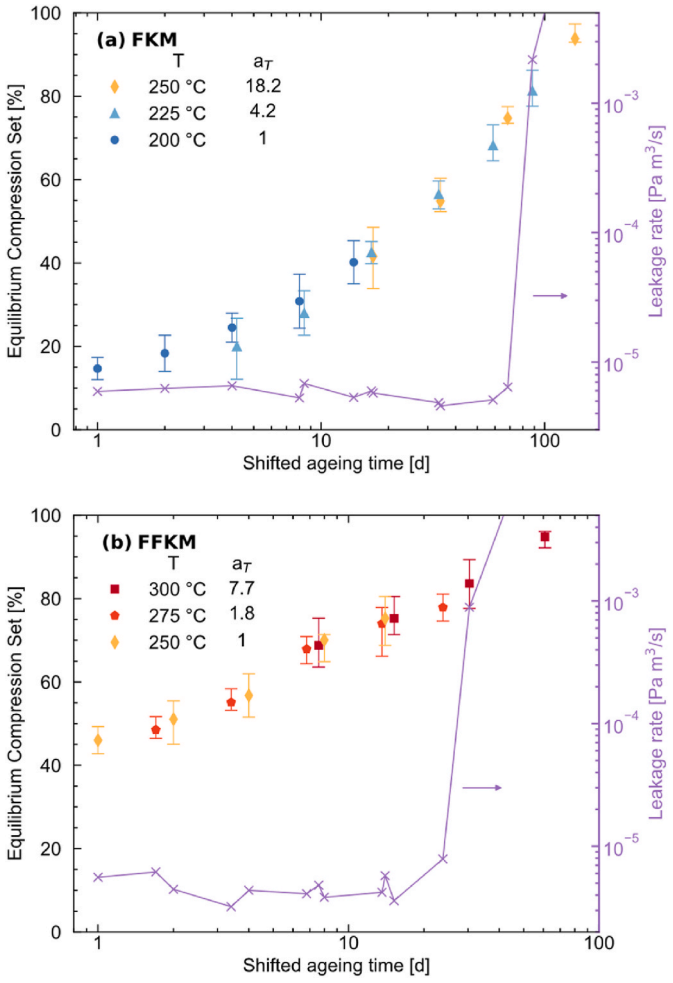

Fig. 17. Master curves and corresponding shift factors (a_T) of equilibrium CS data and corresponding measured leakage rate on secondary axis. Reference temperature for (a) FKM is 200 °C, and for (b) FFKM is 250 °C.

[6,62].

For the FFKM, a less adequate linear fit was found, resulting in an apparent E_a of 110 kJ/mol. Further ageing tests of FFKM O-rings at other temperatures e.g. 325 °C or 225 °C are suggested in order to improve the interpretation of the linear fit and capture if the contribution of the underlying degradation mechanisms change in the examined temperature range. This further investigation would also help determine whether the nonlinear behaviour persists and if the temperature-dependent degradation process is more appropriately described by a power law model. A reported E_a value for a similar high temperature resistance FFKM was found to be 251 kJ/mol for experiments performed in a TGA aiming for 5 % weight loss in a temperature range of 350–416 °C [27]. Similarly as before, this E_a cannot be directly compared to the one obtained in this work, due to the different testing methods employed and the large temperature differences between the studies, since polymer systems will show several apparent activation energies over a large temperature range. The found E_a for FKM (116 kJ/mol) and for FFKM (110 kJ/mol) reveal that a higher apparent activation energy does not necessarily result in the longest lifetimes, as also reported in literature [4]. Rather, findings suggest that measured parameters such as CS, are more decisive for lifetime prediction than E_a.

Building upon the Arrhenius diagrams discussed previously, it is important to note that our lifetime prediction does not rely on the derived activation energy or extrapolation to lower temperatures. Instead, we employ the time-temperature superposition (TTS) method based on compression set (CS) data, offering a more direct and reliable approach within the measured temperature range. Considering the previously derived end-of-lifetime criterion of 75 % equilibrium CS, the service life of the seals can be determined not only for the temperature where leakage occurred, but also for the other tested ageing temperatures. Even though the guidelines of the DIN ISO 11346 standard [63] for the estimation of lifetime of rubbers permits the extrapolation of the degradation curve up to 30–40 °C beyond the last data point, the lifetime prediction in this study is limited to the tested temperatures to ensure a good accuracy. Table 3 summarizes FKM and FFKM's O-rings empirically derived and predicted times to reach 75 % equilibrium CS and thus reach their end of service. Additionally, the estimated lifetime of FKM and FFKM O-rings at 200 °C on the basis of long-term CSR tests is also reported. These lifetimes were determined as the time required to reach 25 % of the initial sealing force (analogous to 75 % equilibrium CS criterion). The predicted lifetimes for FKM O-rings aged at 200 °C utilising TTS and CSR methods show comparable values with a minor difference of 5 % (73 d vs. 77 d), suggesting good consistency of the results. While the extrapolated data of the TTS master curve leads to a slightly more conservative service lifetime estimate, it reduces testing times considerably by utilising the accelerated ageing approach.

The predicted lifetimes presented in Table 3 consider a 24-h continuous operation of the O-ring seals. However, given that the

Table 3
Empirically derived and predicted lifetimes of FKM and FFKM O-rings at several ageing temperatures.

Material	Lifetime [d][a]					
	200 °C		225 °C	250 °C	275 °C	300 °C
FKM	73	77[b]	17	4		
FFKM		135[b]		16	9	2

[a] Considering 75 % equilibrium CS as end-of-life criterion.
[b] Measured time to reach 25 % of initial sealing force using CSR.

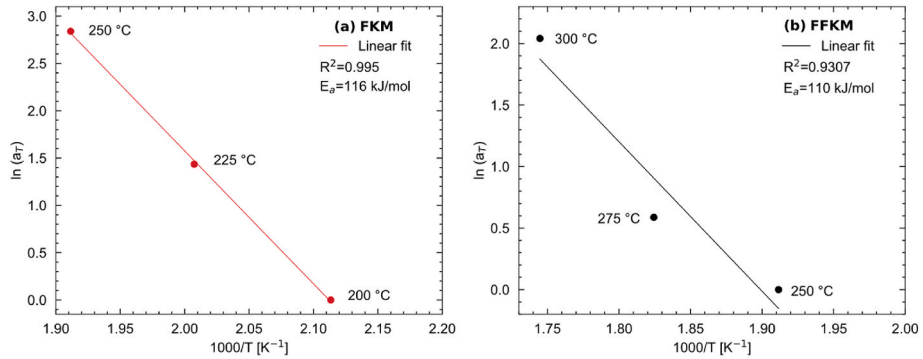

Fig. 18. Arrhenius diagrams of shift factors a_T for (a) FKM and (b) FFKM.

target application is a solar receiver-reactor, operating hours per day are reduced to 8 h to account for sunlight availability. Under these conditions, FKM O-rings achieve lifetimes of 219, 51 and 12 operational days at 200 °C, 225 °C and 250 °C, respectively, while FFKM O-rings attain lifetimes of 405, 48, 27 and 6 operational days at 200 °C, 250 °C, 275 °C and 300 °C, respectively. Operating the O-ring seals at temperatures above 200 °C would require very frequent maintenance intervals (at least once every two months), which is neither economically viable nor operationally desirable, even if performed at night. Therefore, to limit seal replacement frequency, 200 °C is recommended as the operating temperature of the O-ring seals. Indeed, based on the derived service lifetimes of FFKM O-rings at 200 °C and 250 °C, operation at 225 °C may be feasible. However, due to the lack of experimental data collected at this temperature, a conservative operating temperature of 200 °C has been selected. Given the suitability and prolonged stability of both elastomers, FKM and FFKM, at 200 °C, the material selection decision could either optimize for lower maintenance demands or reduced initial capital expenditures considering the significantly higher price of FFKM. Nevertheless, additional research is needed to evaluate the effects of daily temperature cycling (from ambient to operational conditions) on the O-rings' lifetime. Furthermore, the presented results are valid for the studied FKM and FFKM O-rings, however it is likely that these findings are specific to the used seals' geometry and testing procedure. Further testing may be required to validate the derived correlations with other elastomeric materials and O-ring dimensions.

4. Conclusions

The degradation of FKM and FFKM O-rings at high temperatures between 200 °C and 300 °C has been studied by analysing the structural and mechanical changes of the elastomers upon thermo-oxidative ageing. Aged FKM O-rings display a significant change in colour from blue in the unexposed case through greyish and finally brownish for the samples aged at the highest temperatures and longest times. Aged samples also displayed the evolution of heterogeneities, softening, adhesion and pronounced surface roughness. IR measurements of aged samples suggest that FKM's degradation results from the thermally activated elimination of hydrofluoric acid from the $–CF_2$ group, leading to newly formed C=C double bonds. The oxidation of C=C double bonds to carbonyl functionalities is evidenced and associated with chain scission and backbone cleavage. Through the accelerated ageing programme FKM O-rings exhibit a minimal increase in hardness, and a high equilibrium compression set (CS) with increasing temperatures and longer exposure times.

With thermo-oxidative ageing, FFKM O-rings displayed material bulging at the edges of the seal suggesting pronounced material softening. At the point of seal failure, crevices and O-ring diameter's deformation (Fig. 3 (d)) are observed. Based on IR data, it is suggested that during thermo-oxidative ageing, CF_2 groups are eliminated as a result of a C–C bond break in the main chain. Findings also suggest that a radical reaction and post-curing processes resulting in additional crosslinking might also occur during material ageing. Chain scission reactions lead to a decrease in hardness of the thermo-oxidatively aged samples as evidenced during testing. FFKM O-rings show higher equilibrium CS for short exposure times but display a higher temperature resistance than FKM at 250 °C. Long-term (5-month) compression stress relaxation (CSR) tests were carried out at 200 °C for both elastomers, where FFKM showed better long-term ageing resistance.

Leakage rate tests of thermo-oxidatively aged FKM and FFKM O-rings were performed, and failure of the sealing system was evidenced to occur in a sudden manner, rather than progressively. Equilibrium CS data is extrapolated using time-temperature shifts (TTS) and used to derive an end-of-life criterion which correlates the elastomers' CS changes to leakage rates above a determined threshold. The end-of-life criterion was conservatively estimated to be 75 % equilibrium CS and is used to perform service lifetime predictions of FKM and FFKM O-rings at several temperatures. FKM O-rings' lifetimes are 73, 17 and 4 days at 200 °C, 225 °C and 250 °C, respectively. While FFKM O-rings' lifetimes are 135 (determined by CSR), 16, 9 and 2 days at 200 °C, 250 °C, 275 °C and 300 °C, respectively. However, longer lifetimes can perhaps be achieved when the O-ring deformation is adjusted according to the elevated working temperature, thus reducing mechanical stress during the ageing process. Considering an 8-h operation window per day (usual for solar applications), findings suggest that service lifetimes in the range of 200 days for FKM and 400 days for FFKM are attainable when operating at 200 °C, making either of the studied elastomers well-suited for the application. On the other hand, gate operating temperatures above 200 °C are not recommended, as the O-rings' significantly reduced lifetimes would translate into highly frequent maintenance requirements, posing economic and operational challenges to the solar reactor's operation.

CRediT authorship contribution statement

Estefanía Vega Puga: Writing – review & editing, Writing – original draft, Validation, Methodology, Investigation, Formal analysis, Conceptualization. **Volker Wachtendorf:** Writing – review & editing, Writing – original draft, Validation, Investigation, Formal analysis. **Anja Kömmling:** Writing – review & editing, Visualization, Supervision, Methodology, Conceptualization. **Stefan Brendelberger:** Writing – review & editing, Supervision, Project administration, Methodology, Conceptualization. **Matthias Jaunich:** Writing – review & editing, Visualization, Resources, Methodology, Conceptualization. **Christian Sattler:** Supervision, Resources, Funding acquisition.

Declaration of AI-assisted technologies in the writing process

During the preparation of this work the authors used DeepL in order to improve the readability and language. After using this tool/service, the authors reviewed and edited the content as needed and take full responsibility for the content of the published article.

Declaration of competing interest

The authors declare that they have no known competing financial interests or personal relationships that could have appeared to influence the work reported in this paper.

Acknowledgements

We would like to thank Mr. Y. Wägner, BAM, for conducting the IR-microscopic measurements.

The project on which this report is based was co-funded by the German Federal Ministry for Economics and Climate Action under the funding code Redox3D (03EE5124A) and the DLR's basic funding under the SOLHYKO project. The authors are responsible for the content of this publication.

Data availability

Data will be made available on request.

References

[1] J.G. Drobny, Fluoroelastomers Handbook: the Definitive User's Guide, William Andrew Publishing, Oxford, UK, 2016.

[2] S. Brendelberger, P. Holzemer-Zerhusen, E. Vega Puga, M. Roeb, C. Sattler, Study of a new receiver-reactor cavity system with multiple mobile redox units for solar thermochemical water splitting, Sol. Energy 235 (2022) 118–128, https://doi.org/10.1016/j.solener.2022.02.013.

[3] E. Vega Puga, S. Brendelberger, A. Weber, C. Sattler, Modeling development of a receiver–reactor of type R2Mx for thermochemical water splitting, J. Sol. Energy Eng. 146 (5) (2024) 51011, https://doi.org/10.1115/1.4065975.

[4] A. Kömmling, M. Jaunich, M. Goral, D. Wolff, Insights for lifetime predictions of O-ring seals from five-year long-term aging tests, Polym. Degrad. Stabil. 179 (2020) 109278, https://doi.org/10.1016/j.polymdegradstab.2020.109278.

[5] A. Kömmling, M. Jaunich, P. Pourmand, D. Wolff, M. Hedenqvist, Analysis of O-ring seal failure under static conditions and determination of end-of-lifetime criterion, Polymers 11 (8) (2019), https://doi.org/10.3390/polym11081251.

[6] A. Kömmling, M. Jaunich, P. Pourmand, D. Wolff, U.W. Gedde, Influence of ageing on sealability of elastomeric O-rings, Macromol. Symp. 373 (1) (2017), https://doi.org/10.1002/masy.201600157.

[7] S. Mitra, A. Ghanbari-Siahkali, P. Kingshott, K. Almdal, H. Kem Rehmeier, A. G. Christensen, Chemical degradation of fluoroelastomer in an alkaline environment, Polym. Degrad. Stabil. 83 (2) (2004) 195–206, https://doi.org/10.1016/S0141-3910(03)00235-0.

[8] K. Surve, M. Cai, J. Yun, A. Zolfaghari, R. Krishnamoorti, A.K. Bhowmick, Effect of extreme environments on aging of fluoroelastomers, Polym. Degrad. Stabil. 227 (2024) 110875, https://doi.org/10.1016/j.polymdegradstab.2024.110875.

[9] T. Sugama, T. Pyatina, E. Redline, J. McElhanon, D. Blankenship, Degradation of different elastomeric polymers in simulated geothermal environments at 300 °C, Polym. Degrad. Stabil. 120 (2015) 328–339, https://doi.org/10.1016/j.polymdegradstab.2015.07.010.

[10] Erica Marie Redline, Mathias C. Celina, Toshifumi Sugama, Tatiana Pyatina, "Evaluation of High Temperature Elastomers for Geothermal Wells." SAND2015-9580, Sandia National Laboratories, Albuquerque, NM, 2015, https://doi.org/10.2172/1504859. https://www.osti.gov/biblio/1504859, journal =.

[11] Qi-Long Wang, Pei, Li Jing-Ke, Gao, Xi He, Yan-Hua Niu, Guang-Xian Li, Accelerated aging behaviors and mechanism of fluoroelastomer in lubricating oil medium, Chin. J. Polym. Sci. 38 (8) (2020) 853–866, https://doi.org/10.1007/s10118-020-2410-1.

[12] G. Yang, Q. Wang, W. Zhuo, G. Li, Y. Niu, Gu Li, Oxidation of lubricating oil and its influence on the aging behaviors of fluorine rubber, J. Appl. Polym. Sci. 140 (5) (2023) e53402, https://doi.org/10.1002/app.53402.

[13] M.A. Kader, A.K. Bhowmick, Thermal ageing, degradation and swelling of acrylate rubber, fluororubber and their blends containing polyfunctional acrylates, Polym. Degrad. Stabil. 79 (2) (2003) 283–295, https://doi.org/10.1016/S0141-3910(02)00292-6.

[14] D. Bulut, T. Krups, G. Poll, U. Giese, Lubricant compatibility of FKM seals in synthetic oils, Ind. Lubric. Tribol. 72 (5) (2020) 557–565, https://doi.org/10.1108/ILT-02-2019-0065.

[15] A. Zolfaghari, J. Yun, V. Singh, Operational envelope prediction of fluoroelastomer seals for downhole operation in the oil and gas industry, J. Appl. Polym. Sci. 139 (5) (2022) 51575, https://doi.org/10.1002/app.51575.

[16] M. Rinnbauer, E. Osen, M. Viol, V. Peterseim, FKM sealings for alternative fuel mixtures, MTZ worldwide 69 (4) (2008) 28–31, https://doi.org/10.1007/BF03226901.

[17] S. Akhlaghi, A.M. Pourrahimi, C. Sjöstedt, M. Bellander, M.S. Hedenqvist, U. W. Gedde, Degradation of fluoroelastomers in rapeseed biodiesel at different oxygen concentrations, Polym. Degrad. Stabil. 136 (2017) 10–19, https://doi.org/10.1016/j.polymdegradstab.2016.12.006.

[18] A. Simon, J. Pepin, D. Berthier, S. Méo, Degradation mechanism of FKM during thermo-oxidative aging from mechanical and network structure correlations, Polym. Degrad. Stabil. 208 (2023) 110271, https://doi.org/10.1016/j.polymdegradstab.2023.110271.

[19] M. Zaghdoudi, A. Kömmling, M. Böhning, M. Jaunich, Ageing of elastomers in air and in hydrogen environment: a comparative study, Int. J. Hydrogen Energy 63 (2024) 207–216, https://doi.org/10.1016/j.ijhydene.2024.03.053.

[20] T.S. Reger, G.J. Reichl, Science of sealing: advanced materials for high-temperature applications. 31st Annual SEMI Advanced Semiconductor Manufacturing Conference (ASMC), August 24–26, 2020, pp. 1–5, https://doi.org/10.1109/ASMC49169.2020.9185380. Saratoga Springs, NY, USA.

[21] W.Y. Zhuo, Q.L. Wang, G. Li, G. Yang, H. Zhang, W. Xu, Y.H. Niu, G.X. Li, Detection of the destruction mechanism of perfluorinated elastomer (FFKM) network under thermo-oxidative aging conditions, Chin. J. Polym. Sci. 40 (5) (2022) 504–514, https://doi.org/10.1007/s10118-022-2692-6.

[22] J.G. Drobny, S. Ebnesajjad, Technology of Fluoropolymers: A Concise Handbook, CRC Press, Boca Raton, 2023.

[23] W. Hofmann, Rubber Technology Handbook, Carl Hanser Verlag, Munich, 1989.

[24] R.C. Klingender, Handbook of Specialty Elastomers, CRC Press, Boca Raton, 2008.

[25] Solvay Solexis, Tecnoflon: a guide to fluoroelastomers. http://20.210.105.67/research/wp-content/uploads/2008/11/fkm_guide_rev113004.pdf, 2005.

[26] Dupont, Perfluoroelastomer (FFKM) and fluoroelastomer (FKM) seals for photovoltaic cell manufacturing processes, Technical Information—Rev. 1, Paper Presented at InterSolar SMET 2009, Munich (2010), in: https://www.dupont.com/content/dam/dupont/amer/us/en/kalrez/public/documents/en/Perfluoroelastomer_and_Fluoroelastomer_Seals_for_Photovoltaic_Cell_Manufacturing_Processes.pdf.

[27] A. Verschuere, E. Cole, FFKM to overcome new challenges: an introduction to perfluoroelastomers, Rubber Fibres Plastics Intl 10 (2) (2015) 122–129.

[28] C. Otto Gehrckens GmbH, K.G. Co, Technisches Datenblatt Vi 665, COG, Pinnenberg, Germany, 2024. https://www.cog.de/uploads/tx_datenblattgenerator/pdf/de/vi-665.pdf.

[29] C. Otto Gehrckens GmbH & Co. KG, Technisches Datenblatt Perlast G75B, COG, Pinnenberg, Germany, 2021. https://www.cog.de/uploads/tx_datenblattgenerator/pdf/de/perlast-g75b.pdf.

[30] ASTM D 1418:2022, Standard Practice for Rubber and Rubber Latices-Nomenclature, ASTM International, USA, 2022.

[31] K.T. Gillen, R. Bernstein, M. Celina, Challenges of acceletrated ageing techniques for elastomer lifetime predictions, Rubber Chem. Technol. 88 (1) (2015) 1–27, https://doi.org/10.5254/rct.14.85930.

[32] K.T. Gillen, R.L. Clough, Rigorous experimental confirmation of a theoretical model for diffusion-limited oxidation, Polymer 33 (20) (1992) 4358–4365, https://doi.org/10.1016/0032-3861(92)90280-A.

[33] J. Wise, K.T. Gillen, R.L. Clough, Quantitative model for the time development of diffusion-limited oxidation profiles, Polymer 38 (8) (1997) 1929–1944, https://doi.org/10.1016/S0032-3861(96)00716-1.

[34] M.D. Hoffman, Dynamic mechanical signatures of Viton A and plastic bonded explosives based on this polymer, Polym. Eng. Sci. 43 (1) (2003) 139–156, https://doi.org/10.1002/pen.10012.

[35] ISO 188, Rubber, Vulcanized or Thermoplastic — Accelerated Ageing and Heat Resistance Tests, International Organization for Standarization, Geneva, Switzerland, 2023. https://www.iso.org/standard/80468.html.

[36] ISO 48-4, Rubber, Vulcanized or Thermoplastic — Determination of Hardness: Part 4: Indentation Hardness by Durometer Method (Shore Hardness), International Organization for Standarization, Geneva, Switzerland, 2018. https://www.iso.org/standard/74969.html.

[37] ISO 815-1, Rubber, vulcanized or thermoplastic — determination of compression set: Part 1: at ambient or elevated temperatures, International Organization for Standarization, Geneva, Switzerland, 2019. https://www.iso.org/standard/74943.html.

[38] ISO 3384-1, Rubber, vulcanized or thermoplastic — determination of stress relaxation in compression, International Organization for Standarization, Geneva, Switzerland, 2024. https://www.iso.org/standard/86478.html.

[39] Vega Puga, E., Brendelberger, S., Pierno, F., Wischek, J., and Sattler, C., "Sealability analysis of aged elastomer O-rings for usage in solar thermochemical water-splitting reactors.", 5th International Congress on Advanced Materials Sciences and Engineering (AMSE), p. 1–5, Lovran, Croatia, July 23–26, Accepted.

[40] I. Song, T. Lee, K. Ryu, Y. Kim, K. Jin, S. Myung, J.W. Park, J.H. Kim, Effects of heat and gamma radiation on the degradation behaviour of fluoroelastomer in a simulated severe accident environment, Nucl. Eng. Technol. 54 (12) (2022) 4514–4521, https://doi.org/10.1016/j.net.2022.08.006.

[41] P.-C. Lee, S.Y. Kim, Y.K. Ko, J.U. Ha, S.K. Jeoung, J.-Y. Lee, M. Kim, Durability and service life prediction of fluorocarbon elastomer under thermal environments, Polymers 14 (10) (2022) 1–11, https://doi.org/10.3390/polym14102047.

[42] Z. Zhang, T. Liang, Z. Jiang, X. Jiang, J. Hu, G. Pang, Application of infrared spectroscopy in research on aging of silicone rubber in harsh environment, Polymers 14 (21) (2022), https://doi.org/10.3390/polym14214728.

[43] J. Mihaly, S. Sterkel, H. Ortner, L. Kocsis, L. Hajba, É. Furdyga, J. Mink, FTIR and FT-Raman spectroscopic study on polymer based high pressure digestion vessels, Croat. Chem. Acta 79 (3) (2006).

[44] B.A. Trisna, S. Park, I. Park, J. Lee, J.S. Lim, Measurement report: radiative efficiencies of (CF 3) 2 CFCN, CF 3 OCFCF 2 and CF 3 OCF 2 CF 3, Atmos. Chem. Phys. 23 (7) (2023) 4489–4500, https://doi.org/10.5194/acp-23-4489-2023.

[45] J.A. Hiltz, Characterization of fluoroelastomers by various analytical techniques including pyrolysis gas chromatography/mass spectrometry, J. Anal. Appl. Pyrolysis 109 (2014) 283–295, https://doi.org/10.1016/j.jaap.2013.06.008.

[46] E. Rabinowitch, W.C. Wood, The collison mechanism and the primary photochemical process in solutions, Trans. Faraday Soc. 32 (0) (1936) 1381–1387, https://doi.org/10.1039/TF9363201381.

[47] S.G. Burnay, J.W. Hitchon, Prediction of service lifetimes of elastomeric seals during radiation ageing, J. Nucl. Mater. 131 (2) (1985) 197–207, https://doi.org/10.1016/0022-3115(85)90458-1.

[48] E. Schutte, T.J.R. Weakley, D.R. Tyler, Radical cage effects in the photochemical degradation of polymers: effect of radical size and mass on the cage recombination efficiency of radical cage pairs generated photochemically from the (cpCH2CH2N(CH3)C(O)(CH2)nCH3)2Mo2(CO)6 (n = 3, 8, 18) complexes, J. Am. Chem. Soc. 125 (34) (2003) 10319–10326, https://doi.org/10.1021/ja035030r.

[49] R.D. Andrews, A.V. Tobolsky, E.E. Hanson, The theory of permanent set at elevated temperatures in natural and synthetic rubber vulcanizates, J. Appl. Phys. 17 (5) (1946) 352–361, https://doi.org/10.1063/1.1707724.

[50] A. Kömmling, M. Jaunich, D. Wolff, Revealing effects of chain scission during ageing of EPDM rubber using relaxation and recovery experiment, Polym. Test. 56 (2016) 261–268, https://doi.org/10.1016/j.polymertesting.2016.10.026.

[51] Maha Zaghdoudi, Anja Kömmling, Matthias Jaunich, Dietmar Wolff, Scission, cross-linking, and physical relaxation during thermal degradation of elastomers, Polymers 11 (8) (2019), https://doi.org/10.3390/polym11081280.

[52] E.A. Salazar, J.G. Curro, K.T. Gillen, Physical and chemical stress relaxation of a fluoroelastomer, J. Appl. Polym. Sci. 21 (6) (1977) 1597–1605, https://doi.org/10.1002/app.1977.070210615.

[53] R. Brown, M. Forrest, Long-term and accelerated ageing tests on rubbers. Rapra Technology, 2000.

[54] C. Repplinger, S. Sellen, S. Kedziora, A. Zürbes, S. Maas, Material modeling for numerical simulation of elastomer O-rings with experimental verification at low temperatures, Int. J. Hydrogen Energy 80 (2024) 1046–1061, https://doi.org/10.1016/j.ijhydene.2024.06.427.

[55] ITER, ITER vacuum handbook, ITER-19-004, https://www.iter.org/sites/default/files/media/2024-04/iter_vacuum_handbook.pdf, 2019.

[56] K.T. Gillen, R. Bernstein, M.H. Wilson, Predicting and confirming the lifetime of O-rings, Polym. Degrad. Stabil. 87 (2) (2005) 257–270, https://doi.org/10.1016/j.polymdegradstab.2004.07.019.

[57] Kömmling, A., "Alterung und Lebensdauervorhersage von O-Ring-Dichtungen." Dissertation. TU Berlin, Berlin, Germany, https://doi.org/10.14279/depositonce-5827.

[58] K.T. Gillen, M. Celina, R. Bernstein, Validation of improved methods for predicting long-term elastomeric seal lifetimes from compression stress–relaxation and oxygen consumption techniques, Polym. Degrad. Stabil. 82 (1) (2003) 25–35, https://doi.org/10.1016/S0141-3910(03)00159-9.
[59] J.D. Ferry, Viscoelastic Properties of Polymers, John Wiley and Sons, New York, 1980.
[60] S.H. Kalfayan, R.H. Silver, A.A. Mazzeo, S.T. Liu, Long term aging of elastomers: chemorheology of viton B fluorocarbon elastomer, JPL Quart. Tech. Rev. 2 (3) (1972).
[61] B. Omnes, Arrhenius Seal Life Prediction Project: Results and Analysis, Valve World Publisher, 2023. https://valve-world.net/arrhenius-seal-life-prediction-project-results-and-analysis/.
[62] R.J. Pazur, Activation energy of poly(isobutylene) under thermo-oxidative conditions from 40 to 100 °C, Polym. Degrad. Stabil. 104 (6) (2014) 57–61, https://doi.org/10.1016/j.polymdegradstab.2014.03.028.
[63] ISO 11346, Rubber, Vulcanized or Thermoplastic — Estimation of Life-Time and Maximum Temperature of Use, International Organization for Standarization, Geneva, Switzerland, 2023. https://www.iso.org/standard/80469.html.